

Thrust distribution in Higgs decays up to the fifth logarithmic order

Wan-Li Ju,^a Yongqi Xu,^b Li Lin Yang,^c Bin Zhou^d

^a*INFN, Sezione di Milano, Via Celoria 16, 20133 Milano, Italy*

^b*School of Physics and State Key Laboratory of Nuclear Physics and Technology, Peking University, Beijing 100871, China*

^c*Zhejiang Institute of Modern Physics, School of Physics, Zhejiang University, Hangzhou 310027, China*

^d*INPAC, Shanghai Key Laboratory for Particle Physics and Cosmology, School of Physics and Astronomy, Shanghai Jiao Tong University, Shanghai 200240, China*

E-mail: Wanli.Ju@mi.infn.it, xuyongqi@pku.edu.cn,
yanglilin@zju.edu.cn, zb0429@sjtu.edu.cn

ABSTRACT: In this work, we extend the resummation for the thrust distribution in Higgs decays up to the fifth logarithmic order. We show that one needs the accurate values of the three-loop soft functions for reliable predictions in the back-to-back region. This is especially true in the gluon channel, where the soft function exhibits poor perturbative convergence.

Contents

1	Introduction	2
2	Theoretical framework	2
3	Numeric results	7
3.1	Choice of parameters and estimation of uncertainties	7
3.2	The resummed thrust distributions in the gluon channel	7
3.3	The resummed thrust distributions in the quark-antiquark channel	10
4	Summary and outlook	10
A	Choice of scales in the momentum space	11
B	Fixed order ingredients	14
C	Anomalous dimensions	20

1 Introduction

The hadronic decays of the Higgs boson provide a unique windows to study the Yukawa couplings of the lighter quarks such as the charm quark and the strange quark. These rare decays might be enhanced by new physics effects beyond the standard model (see, e.g., [1, 2]), and can be probed at the Large Hadron Collider (LHC) and the future Higgs factories [3–7]. However, the hadronic decays of the Higgs boson can also proceed through the $H \rightarrow gg$ partonic channel. While the gluon channel is also useful, it is desirable to distinguish it from the $H \rightarrow q\bar{q}$ channel to gain maximal information about the Yukawa couplings. To this end, it is important to study various differential distributions in these two channels.

A classical differential distribution for hadronic final states is the event shape variable “thrust” [8]. It was extensively studied in the process $e^+e^- \rightarrow$ hadrons. In the context of $H \rightarrow$ hadrons, the next-to-leading order (NLO) and approximate next-to-next-to-leading order (NNLO) predictions were calculated in [9]. These fixed-order results suffer from large logarithms in the endpoint region, which need to be resummed to all orders in the strong coupling α_s . The resummation framework is also well-established for $e^+e^- \rightarrow$ hadrons [10–18]. The applications to the Higgs case were carried out in [19, 20] at the next-to-next-to-leading logarithmic (NNLL and NNLL’) accuracies. In this work, we extend the resummation accuracy up to the fifth order, and present the results at N³LL’ and N⁴LL.

The paper is organized as follows. In Section 2 we briefly review the factorization formula for the thrust distribution, and give technical details of the resummation framework. In Section 3 we provide numeric results for the resummed thrust distributions, with jet and soft scales chosen in the Laplace space. The summary and outlook come in Section 4. The alternative results with jet and soft scales chosen in the momentum space are presented in Appendix A, and we leave some lengthy expressions to the remaining Appendices.

2 Theoretical framework

We consider the process $H \rightarrow$ hadrons induced by the following effective Lagrangian

$$\begin{aligned} \mathcal{L}_{\text{eff}} &= \frac{\alpha_s(\mu)C_t(m_t, \mu)}{12\pi v} O_g + \sum_q \frac{y_q(\mu)}{\sqrt{2}} O_q \\ &\equiv \frac{\alpha_s(\mu)C_t(m_t, \mu)}{12\pi v} H G^{\mu\nu, a} G_{\mu\nu}^a + \sum_q \frac{y_q(\mu)}{\sqrt{2}} H \bar{\psi}_q \psi_q, \end{aligned} \quad (2.1)$$

where v is the Higgs vacuum expectation value; H represents the physical Higgs boson after electroweak symmetry breaking; $G_{\mu\nu}^a$ is the field strength tensor of the gluon field; ψ_q represent the light quark fields. We will ignore the masses of the light quarks, but keep the Yukawa couplings y_q non-vanishing. The strong coupling α_s , the Yukawa coupling y_q and the Wilson coefficient C_t of the effective operator are renormalized in the $\overline{\text{MS}}$ scheme at the scale μ .

The thrust variable T is defined as

$$T \equiv \max_{\vec{n}} \frac{\sum_i |\vec{n} \cdot \vec{p}_i|}{\sum_i |\vec{p}_i|}, \quad (2.2)$$

where \vec{p}_i denote the 3-momenta of final state particles. The unit vector \vec{n} that maximize the above ratio is called the thrust axis. For convenience we introduce the variable $\tau \equiv 1 - T$. In this work we are concerned with the limit $T \rightarrow 1$ or $\tau \rightarrow 0$. Physically this corresponds to two back-to-back jets in the final state. In this limit the differential decay rate can be factorized into the product (convolution) of a hard function, a soft function and two jet functions [9–12, 21–24]:

$$\begin{aligned}\frac{d\Gamma^q}{d\tau} &= \Gamma_B^q(\mu) |C_S^q(m_H, \mu)|^2 \int dp_n^2 dp_{\bar{n}}^2 dk \delta\left(\tau - \frac{p_n^2 + p_{\bar{n}}^2}{m_H^2} - \frac{k}{m_H}\right) \\ &\quad \times J_n^q(p_n^2, \mu) J_{\bar{n}}^q(p_{\bar{n}}^2, \mu) S^q(k, \mu), \\ \frac{d\Gamma^g}{d\tau} &= \Gamma_B^g(\mu) |C_t(m_t, \mu)|^2 |C_S^g(m_H, \mu)|^2 \int dp_n^2 dp_{\bar{n}}^2 dk \delta\left(\tau - \frac{p_n^2 + p_{\bar{n}}^2}{m_H^2} - \frac{k}{m_H}\right) \\ &\quad \times J_n^g(p_n^2, \mu) J_{\bar{n}}^g(p_{\bar{n}}^2, \mu) S^g(k, \mu),\end{aligned}\quad (2.3)$$

where the superscript q or g labels the partonic subprocesses $H \rightarrow q\bar{q}$ or $H \rightarrow gg$, with Γ_B^q and Γ_B^g being the corresponding total decay rates at the Born level. Their explicit expressions are

$$\Gamma_B^q = \frac{y_q^2(\mu) m_H C_A}{16\pi}, \quad \Gamma_B^g = \frac{\alpha_s^2(\mu) m_H^3}{72 \pi^3 v^2}. \quad (2.4)$$

In the factorization formula, C_S^i (with $i = q, g$) are hard Wilson coefficients arising when matching the full theory of QCD to the soft-collinear effective theory (SCET) [25–30]; S^i are soft functions defined as the vacuum expectation values of soft Wilson-loop operators; J_n^i and $J_{\bar{n}}^i$ are jet functions along the two light-like directions $n^\mu = (1, \vec{n})$ and $\bar{n}^\mu = (1, -\vec{n})$, where \vec{n} is the thrust axis.

The various ingredients satisfy renormalization group (RG) equations

$$\begin{aligned}\frac{d}{d \ln \mu} y_q(\mu) &= \gamma_y(\alpha_s(\mu)) y_q(\mu), \\ \frac{d}{d \ln \mu} C_t(m_t, \mu) &= \gamma_t(\alpha_s(\mu)) C_t(\mu^2), \\ \frac{d}{d \ln \mu} C_S^i(m_H, \mu) &= \left[\Gamma_{\text{cusp}}^i(\alpha_s(\mu)) \ln \frac{-m_H^2 - i\epsilon}{\mu^2} + \gamma_H^i(\alpha_s(\mu)) \right] C_S^i(m_H, \mu), \\ \frac{d}{d \ln \mu} J^i(p^2, \mu) &= \left[-2\Gamma_{\text{cusp}}^i(\alpha_s(\mu)) \ln \frac{p^2}{\mu^2} - 2\gamma_J^i(\alpha_s(\mu)) \right] J^i(p^2, \mu) \\ &\quad + 2\Gamma_{\text{cusp}}^i(\alpha_s(\mu)) \int_0^{p^2} dq^2 \frac{J^i(p^2, \mu) - J^i(q^2, \mu)}{p^2 - q^2}, \\ \frac{d}{d \ln \mu} S^i(k, \mu) &= \left[4\Gamma_{\text{cusp}}^i(\alpha_s(\mu)) \ln \frac{k}{\mu} - 2\gamma_S^i(\alpha_s(\mu)) \right] S^i(k, \mu) \\ &\quad - 4\Gamma_{\text{cusp}}^i(\alpha_s(\mu)) \int_0^k dq \frac{S^i(k, \mu) - S^i(q, \mu)}{k - q}.\end{aligned}\quad (2.5)$$

Note that the evolution equations for the jet and soft functions involve convolutions. It is useful to introduce the Laplace transformed functions

$$\tilde{j}^i(L_J, \mu) = \int_0^\infty dp^2 \exp\left(-\frac{Np^2}{m_H^2}\right) J^i(p^2, \mu),$$

$$\tilde{s}^i(L_S, \mu) = \int_0^\infty dk \exp\left(-\frac{Nk}{m_H}\right) S^i(k, \mu), \quad (2.6)$$

where

$$L_J = \ln \frac{m_H^2}{\mu^2 \bar{N}}, \quad L_S = \ln \frac{m_H}{\mu \bar{N}}, \quad (2.7)$$

with $\bar{N} \equiv N e^{\gamma_E}$ and γ_E being the Euler's constant. The Laplace-space jet and soft functions satisfy local RG equations

$$\begin{aligned} \frac{d}{d \ln \mu} \tilde{j}^i(L_J, \mu) &= [-2\Gamma_{\text{cusp}}^i(\alpha_s(\mu))L_J - 2\gamma_J^i(\alpha_s(\mu))] \tilde{j}^i(L_J, \mu), \\ \frac{d}{d \ln \mu} \tilde{s}^i(L_S, \mu) &= [4\Gamma_{\text{cusp}}^i(\alpha_s(\mu))L_S - 2\gamma_S^i(\alpha_s(\mu))] \tilde{s}^i(L_S, \mu). \end{aligned} \quad (2.8)$$

Under the Laplace transform, the differential decay rates are expressed as

$$\begin{aligned} \int_0^\infty d\tau e^{-\tau N} \frac{d\Gamma^q}{d\tau} &= \Gamma_B^q(\mu) |C_S^q(m_H, \mu)|^2 [\tilde{j}^q(L_J, \mu)]^2 \tilde{s}^q(L_S, \mu), \\ \int_0^\infty d\tau e^{-\tau N} \frac{d\Gamma^g}{d\tau} &= \Gamma_B^g(\mu) |C_t(m_t, \mu)|^2 |C_S^g(m_H, \mu)|^2 [\tilde{j}^g(L_J, \mu)]^2 \tilde{s}^g(L_S, \mu). \end{aligned} \quad (2.9)$$

For small τ , the dominant contribution arises from the region of large N . In this case the large logarithms L_J and L_S appear with increasing powers at each order in the perturbative expansions of the jet and soft functions. We will resum these logarithms to all orders in α_s using RG evolution.

In the RG equations, Γ_{cusp}^i are the cusp anomalous dimensions, which are known up to the four-loop accuracy [31–34], and their fifth order contributions were estimated in [35]. The beta function governing the running strong coupling is known up to the five-loop order in [36–41]. The anomalous dimension γ^y for the Yukawa coupling is the same as that for the quark masses in the $\overline{\text{MS}}$ scheme, and is known up to the fifth order in [42–46]. The non-cusp anomalous dimension γ_t governing scale evolution of the Wilson coefficient C_t is also known on the fifth level [47–52]. The up-to four-loop results for the remaining anomalous dimensions can be found for γ_H^i in [53–62], for γ_S^i in [63–66], and for γ_J^i in [66–73]. The Wilson coefficient C_t is known up to the four-loop order [49–51, 74–77] and so is the hard sector [55, 57–62, 78] in the factorization of Eq. (2.3). As for the fixed-order expansions of the jet functions and the soft functions, the analytic results are known up to the three-loop order [11, 12, 67–73, 79, 80], with the exception of the scale-independent terms of the three-loop soft function. We collect all these ingredients in the Appendices B and C. They allow us to perform the resummation of large logarithms to the $\text{N}^3\text{LL}'$ order and approximately to the N^4LL order. For the counting of logarithmic orders, we refer to Table 1.

To resum the large logarithms, we choose appropriate scales for each of the functions in the factorization formula, and use the RG equations to evolve them to a common scale. The choice of scales can be done either in the Laplace N -space or in the momentum τ -space. In the following, we present results with scale choices in the Laplace space, while

Logarithmic accuracy	$\Gamma_{\text{cusp}}, \beta$	$\gamma_{t,y,H,j,s}$	$C_t, C_S, \tilde{j}, \tilde{s}$
NNLL'	3-loop	2-loop	2-loop
N ³ LL	4-loop	3-loop	2-loop
N ³ LL'	4-loop	3-loop	3-loop
N ⁴ LL	5-loop	4-loop	3-loop

Table 1. Definitions of the logarithmic orders.

those in the momentum space will be discussed in Appendix A. We choose the scales for the C_t, C_S, \tilde{j} and \tilde{s} functions to be

$$\mu_t = e_t m_t, \quad \mu_h = e_h m_H, \quad \mu_j = e_j \frac{m_H}{\sqrt{N}}, \quad \mu_s = e_s \frac{m_H}{N}, \quad (2.10)$$

where by default we take $e_t = e_h = e_j = e_s = 1$, and we vary them up and down by a factor of two to estimate the associated uncertainties. The resummed differential decay rates in the Laplace space can be written as

$$\begin{aligned} \tilde{\Gamma}^q(N) &= \Gamma_B^q(\mu_h) U^q(\mu_h, \mu_j, \mu_s) |C_S^q(m_H, \mu_h)|^2 [\tilde{j}^q(L_J, \mu_j)]^2 \tilde{s}^q(L_S, \mu_s) \left(\frac{m_H}{\mu_s N} \right)^{\eta_q}, \\ \tilde{\Gamma}^g(N) &= \Gamma_B^g(\mu_h) U^g(\mu_t, \mu_h, \mu_j, \mu_s) |C_t(m_t, \mu_t)|^2 |C_S^g(m_H, \mu_h)|^2 \\ &\quad \times [\tilde{j}^g(L_J, \mu_j)]^2 \tilde{s}^g(L_S, \mu_s) \left(\frac{m_H}{\mu_s N} \right)^{\eta_g}, \end{aligned} \quad (2.11)$$

where the evolution functions are given by

$$\begin{aligned} U^q(\mu_h, \mu_j, \mu_s) &= \exp \left[4S^q(\mu_h, \mu_j) + 4S^q(\mu_s, \mu_j) - 2A_{\text{cusp}}^q(\mu_h, \mu_j) \ln \frac{m_H^2}{\mu_h^2} \right. \\ &\quad \left. - 2A_S^q(\mu_h, \mu_s) - 4A_J^q(\mu_h, \mu_j) \right], \\ U^g(\mu_t, \mu_h, \mu_j, \mu_s) &= \exp \left[2A_t(\mu_h, \mu_t) + 4S^g(\mu_h, \mu_j) + 4S^g(\mu_s, \mu_j) - 2A_{\text{cusp}}^g(\mu_h, \mu_j) \ln \frac{m_H^2}{\mu_h^2} \right. \\ &\quad \left. - 2A_S^g(\mu_h, \mu_s) - 4A_J^g(\mu_h, \mu_j) \right], \end{aligned} \quad (2.12)$$

in which the functions $S^{q,g}$ and $A_i^{q,g}$ are defined by [81]

$$\begin{aligned} S^{q,g}(\nu, \mu) &= - \int_{\alpha_s(\nu)}^{\alpha_s(\mu)} d\alpha_s \frac{\Gamma_{\text{cusp}}^{q,g}(\alpha_s)}{\beta(\alpha_s)} \int_{\alpha_s(\nu)}^{\alpha_s} \frac{d\tilde{\alpha}_s}{\beta(\tilde{\alpha}_s)}, \\ A_i^{q,g}(\nu, \mu) &= - \int_{\alpha_s(\nu)}^{\alpha_s(\mu)} d\alpha_s \frac{\gamma_i^{q,g}(\alpha_s)}{\beta(\alpha_s)}, \end{aligned} \quad (2.13)$$

for $i = \text{cusp}, t, S, J$, and $\eta_{q,g} = 4A_{\text{cusp}}^{q,g}(\mu_j, \mu_s)$. The momentum-space differential decay rates can then be obtained through an inverse Laplace transform

$$\frac{d\Gamma^{q,g}}{d\tau} = \frac{1}{2\pi i} \int_{-i\infty}^{+i\infty} dN e^{N\tau} \tilde{\Gamma}^{q,g}(N). \quad (2.14)$$

The integration contour should, in principle, be chosen such that all singularities of the integrand are situated to the left side. However, the resummed integrand develops a Landau pole at large N due to the scale choices $\mu_j \sim m_H/\sqrt{N}$ and $\mu_s \sim m_H/\bar{N}$, which signals the breakdown of perturbation theory in that region. Correspondingly, the inverse Laplace transform of the perturbatively resummed integrand suffers from an ambiguity of non-perturbative origin. We adopt the so-called Minimal Prescription [82], in which the contour lies to the right of all physical singularities but to the left of the Landau pole.

With the generic framework, we still need to specify a few details in the evaluation of the resummed differential decay rates at a given logarithmic accuracy. The strong coupling α_s at a given scale μ is evaluated according to

$$\begin{aligned} \alpha_s(\mu) = \frac{\alpha_s(\nu)}{X} & \left\{ 1 - \frac{\alpha_s(\nu)}{4\pi X} \frac{\beta_1 \ln(X)}{\beta_0} + \left(\frac{\alpha_s(\nu)}{4\pi X} \right)^2 \left[\frac{\beta_1^2}{\beta_0^2} (\ln^2(X) - \ln(X) - 1 + X) \right. \right. \\ & + \left. \frac{\beta_2}{\beta_0} (1 - X) \right] + \left(\frac{\alpha_s(\nu)}{4\pi X} \right)^3 \left[\frac{\beta_1^3}{\beta_0^3} \left(-\frac{X^2}{2} + X - \ln^3(X) + \frac{5\ln^2(X)}{2} \right. \right. \\ & + \left. 2(1 - X) \ln(X) - \frac{1}{2} \right) + \frac{\beta_3}{2\beta_0} (1 - X^2) + \frac{\beta_1\beta_2}{\beta_0^2} (2X \ln(X) - 3 \ln(X) \\ & - X(1 - X)) \left. \right] + \left(\frac{\alpha_s(\nu)}{4\pi X} \right)^4 \left[-\frac{\beta_4(X^3 - 1)}{3\beta_0} + \frac{\beta_3\beta_1}{6\beta_0^2} ((X - 1)(4X^2 + X + 1) \right. \\ & + 6(X^2 - 2) \ln(X)) + \frac{\beta_2^2(X - 1)^2(X + 5)}{3\beta_0^2} + \frac{\beta_2\beta_1^2}{\beta_0^3} (-(X + 3)(X - 1)^2 \\ & + \ln(X)(-2X^2 + 5X - 3) - 3(X - 2) \ln^2(X)) + \frac{\beta_1^4}{6\beta_0^4} ((X - 1)^2(2X + 7) \\ & \left. \left. + 6 \ln^4(X) - 26 \ln^3(X) + 9(2X - 1) \ln^2(X) + 6(X - 4)(X - 1) \ln(X)) \right] \right\}, \quad (2.15) \end{aligned}$$

where the initial scale is chosen at the Z boson mass, $\nu = m_Z$, and

$$X = 1 + \frac{\alpha_s(\nu)}{2\pi} \beta_0 \ln \frac{\mu}{m_Z}. \quad (2.16)$$

The coefficients of the beta function are defined through

$$\frac{d\alpha_s}{d \ln \mu} = -2\alpha_s \sum_{n=0}^{\infty} \left(\frac{\alpha_s}{4\pi} \right)^{n+1} \beta_n. \quad (2.17)$$

The Yukawa coupling y_q at a given scale is evaluated with

$$y_q(\mu) = y_q(m_H) \exp [A_y^q(\mu, m_H)]. \quad (2.18)$$

The evolution factors $U^{q,g}$ and the factors involving $\eta_{q,g}$ are expanded on the exponent up to a given logarithmic accuracy defined in Table 1. The expansion is done by counting the large logarithms $\ln(\nu/\mu)$ as $\mathcal{O}(1/\alpha_s)$. The fixed-order factors ($|C_S^q|^2 [\tilde{j}^q]^2 \tilde{s}^q$ and $|C_t|^2 |C_S^g|^2 [\tilde{j}^g]^2 \tilde{s}^g$) are also expanded up to a given loop order. We are now ready to perform numeric evaluations of the resummed differential decay rates. The results are presented in the next Section.

3 Numeric results

3.1 Choice of parameters and estimation of uncertainties

In this section we are devoted to the numeric results. Throughout this paper, we choose $\alpha_s(m_Z) = 0.1181$, $m_H = 125.1$ GeV and $m_t = 172.9$ GeV [83]. The scales are chosen as in Eq. (2.10). Note that this choice is conventional in the small- τ region considered in this work. On the other hand, if one wants to match the resummed distributions to the fixed-order ones, it is necessary to deal with the intermediate regime between the resummation dominated small- τ region and the fixed-order dominated large- τ region. We leave this subtlety to future investigations. We estimate the perturbative uncertainties by varying each of e_t , e_h , e_j and e_s up and down by a factor of two, while keeping the others at their defaults. The resulting variations of the differential decay rates are then added in quadrature.

The scale-independent constant terms of the three-loop soft functions are not known yet. The term in the quark channel was extracted in [71] through a numeric fit to the fixed-order thrust distribution, which has a large uncertainty. In this work we set

$$c_{3q}^S = -19988 \pm 5000, \quad (3.1)$$

and estimate the corresponding variation of the resummed distribution. For the gluon channel we apply the Casimir scaling and set

$$c_{3g}^S = -45433 \pm 11250. \quad (3.2)$$

The five-loop cusp anomalous dimensions are also unknown, with only a rough estimation available [35]. However, we have checked that they only have a rather mild effect on the resummed thrust distributions.

3.2 The resummed thrust distributions in the gluon channel

We now show the resummed thrust distributions in the gluon channel at various logarithmic accuracies. The baseline for comparison is the NNLL' result, that is the state-of-the-art accuracy in the literature (see Refs. [19, 20], although they adopted scale choices in the momentum space).

In Fig. 1, we show the comparison between NNLL' and N³LL, and that between NNLL' and N³LL', for the τ range [0.01, 0.15]. This covers the small- τ and intermediate- τ regions, but cuts out the large- τ region where fixed-order matching would be important. One can see that the N³LL result has a slightly reduced scale uncertainty compared to the NNLL' one. The reduction is most significant in the small- τ region, where resummation effects are expected to be important. The N³LL' result further reduces the scale uncertainty in the intermediate τ region, with the three-loop hard, jet and soft functions included. However, we observe an unusual increase of scale uncertainty in the small τ region, as is clear from the right plot of Fig. 1. It can be seen that the two bands even do not overlap below $\tau \sim 0.03$. This fact can be traced to the unusually large constant term c_{3g}^S of the three-loop soft

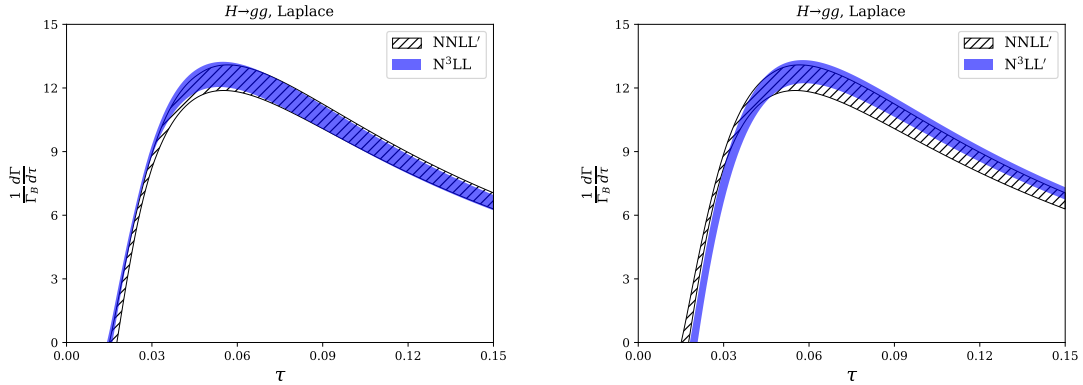


Figure 1. The resummed thrust distributions in the gluon channel. Left: NNLL' vs. N³LL; Right: NNLL' vs. N³LL'.

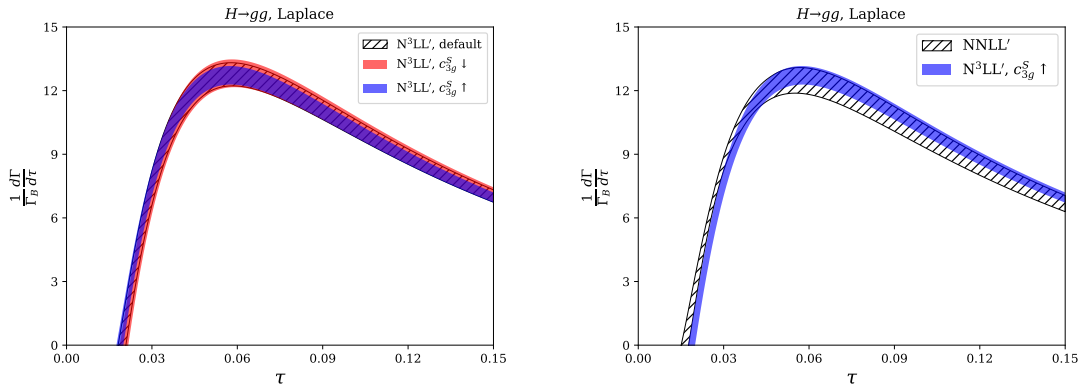


Figure 2. The effects of c_{3g}^S on the N³LL' results in the gluon channel. Left: N³LL' results with 3 values of c_{3g}^S ; Right: NNLL' vs. N³LL' where c_{3g}^S is taken to its “upper” value (with a smaller absolute value).

function. It is instructive to show the soft function at its default scale $\mu_s = m_H/\bar{N}$, where $L_S = 0$, for $c_{3g}^S = -45433$:

$$\tilde{s}^g(0, \mu_s) = 1 - 2.356 \alpha_s(\mu_s) + 1.617 \alpha_s^2(\mu_s) - 22.90 \alpha_s^3(\mu_s) + \dots \quad (3.3)$$

For small τ , one expects that the dominant contributions in the Laplace space come from the region where $\tau N \sim 1$. This means that, below $\tau \sim 0.03$, μ_s is typically only about a few GeVs, where $\alpha_s \sim 0.2$ is not so small. Therefore, the gluon soft function has a rather poor perturbative convergence if we take the fitted central value of c_{3g}^S . It is highly desired to calculate the exact value of c_{3g}^S to settle down this issue: either its absolute value is in fact smaller, and the N³LL' result is already sufficient; or it is indeed that large, then one needs to have even higher order corrections for reliable predictions. Efforts towards this goal are being actively pursued in the literature [84, 85].

To demonstrate the effects of different values of c_{3g}^S , we show in the left plot of Fig. 2

$H \rightarrow gg, \text{N}^3\text{LL}'$	μ_t	μ_h	μ_j	μ_s	c_{3g}^S
max	12.128	12.120	12.120	13.077	12.219
min	12.106	11.967	12.063	12.044	12.020

Table 2. Variations of the $\text{N}^3\text{LL}'$ differential decay rate at $\tau = 0.05$ induced by changing the scales and c_{3g}^S . The central value is 12.120.

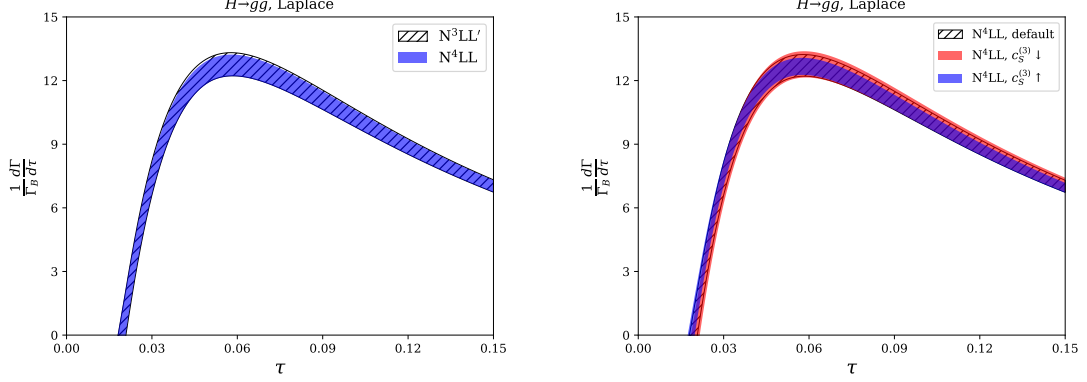


Figure 3. The resummed thrust distributions in the gluon channel. Left: $\text{N}^3\text{LL}'$ vs N^4LL ; Right: N^4LL results with 3 values of c_{3g}^S .

$H \rightarrow gg, \text{N}^4\text{LL}$	μ_t	μ_h	μ_j	μ_s	c_{3g}^S	$\Gamma_{\text{cusp}}^{g(4)}$
max	12.089	12.084	12.084	12.980	12.183	12.085
min	12.073	11.936	12.025	12.022	11.985	12.083

Table 3. Variations of the N^4LL differential decay rate at $\tau = 0.05$ induced by changing the scales, c_{3g}^S and the five-loop cusp anomalous dimension $\Gamma_{\text{cusp}}^{g(4)}$. The central value is 12.084.

the resummed distributions for three values of c_{3g}^S : the default value -45433 , the “lower” value -56683 , and the “upper” value -34183 . Note that since the fitted value of c_{3g}^S is negative, the “upper” value has a smaller absolute value, and leads to a better perturbative convergence. Indeed, as can be seen from the plot, the result with the “upper” value exhibits a smaller scale uncertainty, especially in the small- τ region. It is also evident from the right plot of Fig. 2, that the $\text{N}^3\text{LL}'$ band is better overlapped with the NNLL' one with c_{3g}^S taking the “upper” value. Finally for reference, we list in Table 2 the variations of the $\text{N}^3\text{LL}'$ differential decay rate at $\tau = 0.05$ induced by changing the values of various scales as well as c_{3g}^S . It is clear that the main source of the scale uncertainty comes from the soft scale, as expected. It can also be seen that varying c_{3g}^S has a larger effect than varying μ_t , μ_h or μ_j . All these emphasize again that we need a better understanding of the soft function at and beyond three loops.

We now add another layer of resummation on top of $\text{N}^3\text{LL}'$, and present the results at N^4LL . The results are shown in Fig. 3, with explicit numbers at $\tau = 0.05$ given in Table 3. We find that the additional order of resummation has a mild effect on the distribution,

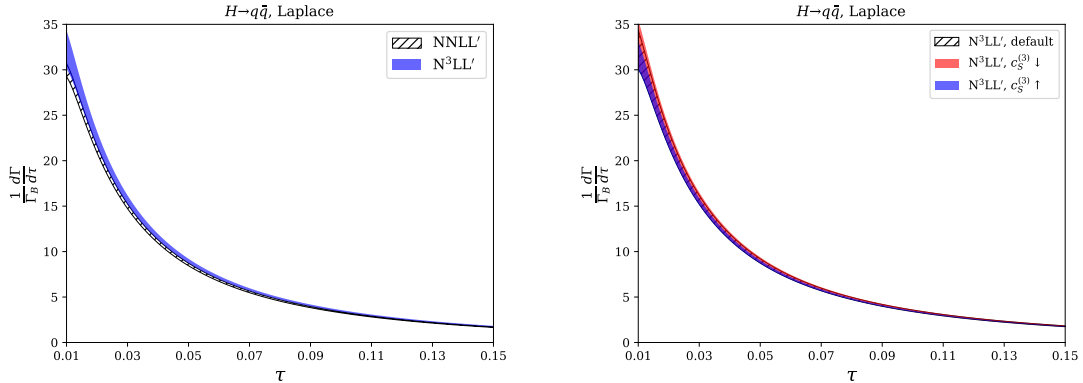


Figure 4. The resummed thrust distributions in the $q\bar{q}$ channel. Left: NNLL' vs. N³LL'; Right: N³LL' results with 3 values of c_{3q}^S .

that is only clearly visible in the peak region. It is also evident that the five-loop cusp anomalous dimension does not have important impacts.

3.3 The resummed thrust distributions in the quark-antiquark channel

We now briefly discuss the results in the quark-antiquark channel. In the left plot of Fig. 4, we compare the NNLL' result against the N³LL' one, where the three-loop constant term c_{3q}^S of the soft function is chosen at the default value. We again observe that the uncertainty band of N³LL' is broader than the NNLL' one, especially at the lower end of the distribution. In the right plot of Fig. 4, we show the N³LL' distributions for 3 values of c_{3q}^S : the default value -19988 , the “upper” value -14988 and the “lower” value -24988 . As expected, the band becomes narrower for the “upper” value, where the absolute value of c_{3q}^S is smaller, and the soft function has a perturbative convergence. Overall, the uncertainties of the resummed thrust distributions in the $q\bar{q}$ channel are significantly smaller than those in the gluon channel. This can be partly explained by the smaller color factor C_F compared to C_A .

4 Summary and outlook

In this work, we extend the resummation for the thrust distribution in Higgs decays up to the fifth logarithmic order. A main conclusion that can be drawn from our results is that one needs the accurate values of the three-loop soft functions for reliable predictions in the small- τ region. This is especially true in the gluon channel, where the perturbative convergence of the soft function seems to be rather bad with a large three-loop constant term.

Once the three-loop soft functions become available, the ingredients collected in this work will allow for faithful numeric predictions at the N³LL' and N⁴LL accuracies. Depending on the size of the three-loop constant, it is possible that one even needs the four-loop gluon soft function to reduce the scale uncertainties and obtain reliable predictions in the small- τ region.

Acknowledgments

This work was supported in part by the National Natural Science Foundation of China under Grant No. 11975030 and 12147103, and the Fundamental Research Funds for the Central Universities.

A Choice of scales in the momentum space

In the main text, we have chosen the jet and soft scales in the Laplace space, and performed the inverse Laplace transform numerically. A different approach is to set the jet and soft scales independent of the Laplace variable N . In this case, the inverse Laplace transform (2.14) can be carried out analytically [12, 81, 86]. For simplicity we only discuss the gluon channel in this Appendix. The result can be written as

$$\begin{aligned} \frac{d\Gamma^g}{d\tau} &= \Gamma_B^g(\mu_h) U^g(\mu_t, \mu_h, \mu_j, \mu_s) |C_t(m_t, \mu_t)|^2 |C_S^g(m_H, \mu_h)|^2 \\ &\times \left[\tilde{j}^g \left(\ln \frac{\mu_s m_H}{\mu_j^2} + \partial_{\eta_g}, \mu_j \right) \right]^2 \tilde{s}^g(\partial_{\eta_g}, \mu_s) \left[\frac{1}{\tau \Gamma(\eta_g)} \left(\frac{\tau m_H}{\mu_s e^{\gamma_E}} \right)^{\eta_g} \right]. \end{aligned} \quad (\text{A.1})$$

The common practice is then to choose μ_s and μ_j as a function of τ , such that $\mu_j \sim \sqrt{\tau} m_H$ and $\mu_s \sim \tau m_H$ in the small- τ region. In this work we don't care about matching with the fixed-order results in the large- τ region (otherwise one needs to introduce ‘‘profile scales’’ as in [19, 20]). Therefore we can adopt the simplest choices

$$\mu_t = e_t m_t, \quad \mu_h = e_h m_H, \quad \mu_j = e_j \sqrt{\tau} m_H, \quad \mu_s = e_s \tau m_H, \quad (\text{A.2})$$

where the parameters e_t , e_h , e_j and e_s are set to 1 by default, and are varied up and down by a factor of two to estimate the uncertainties. The numeric results with the above scale choices are shown in Fig. 5. We observe very large scale uncertainties in the small- τ region, much larger than those seen in Fig. 1. As it turns out, these large uncertainties originate from the jet and soft scales, i.e., e_j and e_s .

The prescription in Eq. (A.2) actually has a subtle problem related exactly to the jet and soft scales. The formula (A.1) is based on the solutions to the RG equations (2.5). Taking the gluon jet function as an example, the RG equation is

$$\begin{aligned} \frac{d}{d \ln \mu} J^g(p^2, \mu) &= \left[-2\Gamma_{\text{cusp}}^g(\alpha_s(\mu)) \ln \frac{p^2}{\mu^2} - 2\gamma_J^g(\alpha_s(\mu)) \right] J^g(p^2, \mu) \\ &+ 2\Gamma_{\text{cusp}}^g(\alpha_s(\mu)) \int_0^{p^2} dq^2 \frac{J^g(p^2, \mu) - J^g(q^2, \mu)}{p^2 - q^2}. \end{aligned} \quad (\text{A.3})$$

And the solution reads [81, 86]

$$J^g(p^2, \mu) = \exp \left[-4S^g(\mu_j, \mu) + 2A_J^g(\mu_j, \mu) \right] \tilde{j}^g(\partial_\eta, \mu_j) \left[\frac{1}{p^2} \left(\frac{p^2}{\mu_j^2} \right)^\eta \right]_* \frac{e^{-\gamma_E \eta}}{\Gamma(\eta)}, \quad (\text{A.4})$$

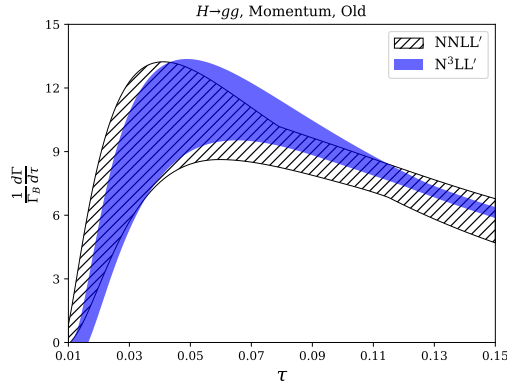


Figure 5. The resummed thrust distributions at NNLL' and N³LL' in the gluon channel with the scale choices (A.2) at the level of differential decay rates.

where $\eta = 2A_{\text{cusp}}^g(\mu_j, \mu)$, and the star-distribution is defined by

$$\int_0^{Q^2} dp^2 \left[\frac{1}{p^2} \left(\frac{p^2}{\mu_j^2} \right)^\eta \right]_* f(p^2) = \int_0^{Q^2} dp^2 \frac{f(p^2) - f(0)}{p^2} \left(\frac{p^2}{\mu_j^2} \right)^\eta + \frac{f(0)}{\eta} \left(\frac{Q^2}{\mu^2} \right)^\eta. \quad (\text{A.5})$$

The solution is of course formally independent of μ_j . However, at any finite order there is a residue dependence. Assuming that μ_j is independent of p^2 , the above solution indeed satisfies the RG equation (A.3), where μ_j is the same in both $J^g(p^2, \mu)$ and $J^g(q^2, \mu)$. However, the scale choice in Eq. (A.2) actually makes μ_j correlated with $p^2 \sim \tau m_H^2$. That is, $\mu_j^2 \sim p^2$ in $J^g(p^2, \mu)$, and $\mu_j^2 \sim q^2$ in $J^g(q^2, \mu)$. This immediately renders the convolution in Eq. (A.3) ill-defined due to the singularity as $q^2 \rightarrow 0$.

One may of course ignore the problem with Eq. (A.3) and insist on using Eq. (A.4) with $\mu_j \sim p^2$ as the resummed jet function. As long as one does not take $p^2 \rightarrow 0$ (where non-perturbative physics enters anyway), this does not pose any difficulty at face value. However, let us take a closer look. We set $\mu_j = e_j \sqrt{p^2}$ in Eq. (A.4), and truncate the solution at NLL' accuracy (that means two-loop Γ_{cusp}^g , one-loop γ_J^g and one-loop \tilde{j}^g). We then expand the resummed jet function in terms of $\alpha_s(\mu)$. This gives

$$J^{g, \text{NLL}'}(p^2, \mu; \mu_j = e_j \sqrt{p^2}) = \frac{\alpha_s(\mu)}{4\pi} \frac{1}{p^2} \left(12 \ln \frac{p^2}{\mu^2} - \frac{23}{3} \right) + \left(\frac{\alpha_s(\mu)}{4\pi} \right)^2 \frac{1}{p^2} \\ \times \left[576 \ln^3(e_j) + 736 \ln^2(e_j) + \left(\frac{9364}{9} - 144\pi^2 \right) \ln(e_j) + 72 \ln^3 \left(\frac{p^2}{\mu^2} \right) + \dots \right] + \mathcal{O}(\alpha_s^3), \quad (\text{A.6})$$

where the ellipsis denotes further e_j -independent terms. We can see that the e_j -dependence cancels at order α_s^1 , as it should at the NLL' accuracy. However, there exist rather high powers of $\ln(e_j)$ at order α_s^2 (and beyond). While $\ln(e_j)$ is counted as a “small” logarithm, these high powers lead to large uncertainties of the resummed jet function when e_j is varied between 1/2 and 2. The resummed soft function $S^g(k, \mu)$ with $\mu_s = e_s k$ exhibits the similar behavior. These explain the large uncertainty bands observed in Fig. 5. In

practice, it is often argued that e_j and e_s are not independent and should be correlated. This can result in partial cancellations between the $\ln^n(e_j)$ and $\ln^n(e_s)$ terms, and lead to smaller uncertainty estimations.

The above behavior does not occur with the scale choices in Eq. (2.10). We can do the same exercise with $\mu_j = e_j m_H / \sqrt{N}$ in the Laplace space. The resummed Laplace-space jet function is given by

$$\tilde{j}^g(L_J, \mu) = \exp[-4S^g(\mu_j, \mu) + 2A_J^g(\mu_j, \mu)] \left(\frac{m_H^2}{N \mu_j^2} \right)^\eta \tilde{j}^g(L_J, \mu_j). \quad (\text{A.7})$$

Again truncating at the NLL' accuracy and expanding in terms of $\alpha_s(\mu)$, we can perform the inverse Laplace transform analytically to arrive at

$$J^{g, \text{NLL}'}(p^2, \mu; \mu_j = e_j m_H / \sqrt{N}) = \frac{\alpha_s(\mu)}{4\pi} \frac{1}{p^2} \left(12 \ln \frac{p^2}{\mu^2} - \frac{23}{3} \right) + \left(\frac{\alpha_s(\mu)}{4\pi} \right)^2 \frac{1}{p^2} \left[72 \ln^3 \left(\frac{p^2}{\mu^2} \right) + \dots \right] + \mathcal{O}(\alpha_s^3). \quad (\text{A.8})$$

Evidently, all the $\ln^n(e_j)$ terms drop out at order α_s^2 . This explains the smaller uncertainty bands in Fig. 1 compared to Fig. 5.

There is an alternative way of choosing the jet and soft scales in the momentum space [18, 87, 88]. We define the accumulative decay rate as

$$\hat{\Gamma}^g(\tau) \equiv \int_0^\tau \frac{d\Gamma^g}{d\tau'} d\tau'. \quad (\text{A.9})$$

In the above integrals, μ_j and μ_s are set to the same expressions as in Eq. (A.2), where τ is the upper bound of the integration. The jet and soft scales are hence independent of the integration variable τ' . Before resummation, the factorization formula for the accumulative decay rates can be obtained by integrating Eq. (2.3) over τ . The result reads

$$\hat{\Gamma}^g(\tau) = \Gamma_B^g(\mu) |C_t(m_t, \mu)|^2 |C_S^g(m_H, \mu)|^2 \int dp_n^2 dp_{\bar{n}}^2 dk \hat{J}_n^g(p_n^2, \mu) \hat{J}_{\bar{n}}^g(p_{\bar{n}}^2, \mu) S^g(k, \mu), \quad (\text{A.10})$$

where the integration domain is determined by the constraints

$$\tau \geq \frac{p_n^2 + p_{\bar{n}}^2}{m_H^2} + \frac{k}{m_H}, \quad p_n^2, p_{\bar{n}}^2, k \geq 0. \quad (\text{A.11})$$

Now, since the jet scale μ_j is a function of τ and is independent of p^2 , the problem with the convolution in Eq. (A.3) is absent here.

After resummation, the accumulative decay rate is

$$\hat{\Gamma}^g(\tau) = \Gamma_B^g(\mu_h) U^g(\mu_t, \mu_h, \mu_j, \mu_s) |C_t(m_t, \mu_t)|^2 |C_S^g(m_H, \mu_h)|^2 \times \left[\tilde{j}^g \left(\ln \frac{\mu_s m_H}{\mu_j^2} + \partial_{\eta_g}, \mu_j \right) \right]^2 \tilde{s}^g(\partial_{\eta_g}, \mu_s) \left[\frac{1}{\Gamma(1 + \eta_g)} \left(\frac{\tau m_H}{\mu_s e^{\gamma_E}} \right)^{\eta_g} \right]. \quad (\text{A.12})$$

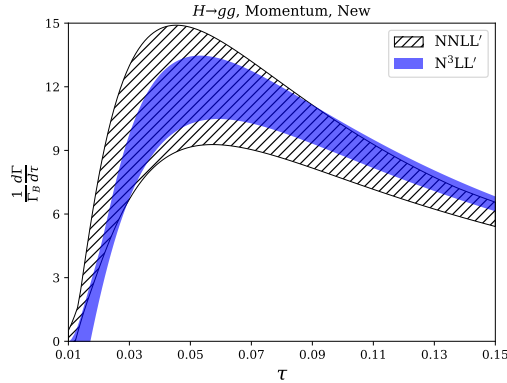


Figure 6. The resummed thrust distributions at NNLL' and N³LL' in the gluon channel with the scale choices (A.2) at the level of accumulative decay rates.

We set the jet and soft scales at the accumulative level following Eq. (A.2), i.e., $\mu_j = e_j \sqrt{\tau} m_H$ and $\mu_s = e_s \tau m_H$. We then take the derivative with respect to τ to obtain the resummed differential decay rate:

$$\frac{d\Gamma^g}{d\tau} = \frac{d}{d\tau} \hat{\Gamma}^g(\tau). \quad (\text{A.13})$$

The numeric results with this new prescription are plotted in Fig. 6.

To compare the “new” way of scale setting at the accumulative level with the “old” way at the differential level, we can study the resummed integrated jet function

$$\begin{aligned} \hat{J}^g(p^2, \mu) &= \int_0^{p^2} dq^2 J^g(q^2, \mu) \\ &= \exp[-4S^g(\mu_j, \mu) + 2A_J^g(\mu_j, \mu)] \tilde{j}^g(\partial_\eta, \mu_j) \left(\frac{p^2}{\mu_j^2}\right)^\eta \frac{e^{-\gamma_E \eta}}{\Gamma(1+\eta)}, \end{aligned} \quad (\text{A.14})$$

with $\mu_j = e_j \sqrt{p^2}$. This is part of the resummed accumulative decay rate (A.12). We still truncate at the NLL' accuracy and expand in terms of $\alpha_s(\mu)$. We then take the derivative with respect to p^2 and arrive at

$$\begin{aligned} \frac{\partial}{\partial p^2} \hat{J}^{g, \text{NLL}'}(p^2, \mu; \mu_j = e_j \sqrt{p^2}) &= \frac{\alpha_s(\mu)}{4\pi} \frac{1}{p^2} \left(12 \ln \frac{p^2}{\mu^2} - \frac{23}{3}\right) \\ &+ \left(\frac{\alpha_s(\mu)}{4\pi}\right)^2 \frac{1}{p^2} \left[72 \ln^3 \left(\frac{p^2}{\mu^2}\right) + \dots\right] + \mathcal{O}(\alpha_s^3). \end{aligned} \quad (\text{A.15})$$

We see that the order α_s^2 term is indeed independent of e_j .

B Fixed order ingredients

In this Appendix we list the fixed-order ingredients appearing in the resummation formula (2.11).

The Wilson coefficient C_t is known up to the four-loop order [47–52]. For our purpose, we need its expression up to three loops, which is given by

$$C_t(m_t, \mu) = 1 + \frac{\alpha_s}{4\pi} 11 + \left(\frac{\alpha_s}{4\pi}\right)^2 \left[L_t \left(19 + \frac{16}{3} n_f \right) + \frac{2777}{18} - \frac{67}{6} n_f \right] \\ + \left(\frac{\alpha_s}{4\pi}\right)^3 \left[L_t^2 \left(209 + 46n_f - \frac{32}{9} n_f^2 \right) + L_t \left(\frac{4834}{9} + \frac{2912}{27} n_f + \frac{77}{27} n_f^2 \right) \right. \\ \left. - \frac{2761331}{648} + \frac{897943\zeta_3}{144} + \left(\frac{58723}{324} - \frac{110779\zeta_3}{216} \right) n_f - \frac{6865}{486} n_f^2 \right], \quad (\text{B.1})$$

where $L_t = \ln(\mu^2/m_t^2)$, and we have explicitly set the number of colors $N_c = 3$ to shorten the expression.

The hard Wilson coefficients $C_S^{q,g}$ are expanded as

$$C_S^{q,g}(m_H, \mu) = \sum_{n=0} \left(\frac{\alpha_s}{4\pi}\right)^n C_S^{q,g(n)}, \quad (\text{B.2})$$

where the gluon channel coefficients up to three-loop order are given by [59]

$$C_S^{g(0)} = 1, \\ C_S^{g(1)} = \left(\frac{\pi^2}{6} - L^2\right) C_A, \\ C_S^{g(2)} = n_f C_A \left[-\frac{2L^3}{9} + \frac{10L^2}{9} + \left(\frac{52}{27} + \frac{2\pi^2}{9}\right) L - \frac{46\zeta_3}{9} - \frac{5\pi^2}{18} - \frac{916}{81} \right] \\ + C_A^2 \left[\frac{L^4}{2} + \frac{11L^3}{9} + \left(\frac{\pi^2}{6} - \frac{67}{9}\right) L^2 + L \left(-2\zeta_3 - \frac{11\pi^2}{9} + \frac{80}{27} \right) - \frac{143\zeta_3}{9} \right. \\ \left. + \frac{\pi^4}{72} + \frac{67\pi^2}{36} + \frac{5105}{162} \right] + n_f C_F \left(2L + 8\zeta_3 - \frac{67}{6} \right), \\ C_S^{g(3)} = n_f C_A C_F \left[-\frac{8L^3}{3} + L^2(13 - 16\zeta_3) + L \left(-\frac{376\zeta_3}{9} + \frac{4\pi^4}{45} + \pi^2 + \frac{3833}{54} \right) \right. \\ \left. + \frac{32\pi^2\zeta_3}{9} + \frac{14564\zeta_3}{81} + \frac{608\zeta_5}{9} - \frac{34\pi^2}{27} - \frac{16\pi^4}{405} - \frac{341219}{972} \right] \\ + n_f^2 C_A \left[-\frac{2L^4}{27} + \frac{40L^3}{81} + \left(\frac{116}{81} + \frac{4\pi^2}{27}\right) L^2 + L \left(-\frac{128\zeta_3}{27} - \frac{40\pi^2}{81} - \frac{14057}{729} \right) \right. \\ \left. + \frac{4576\zeta_3}{243} + \frac{\pi^4}{243} + \frac{2\pi^2}{27} + \frac{611401}{13122} \right] + n_f C_A^2 \left[\frac{2L^5}{9} - \frac{8L^4}{27} + \left(-\frac{734}{81} - \frac{\pi^2}{9} \right) L^3 \right. \\ \left. + L^2 \left(\frac{118\zeta_3}{9} + \frac{377}{27} - \frac{103\pi^2}{54} \right) + L \left(\frac{28\zeta_3}{9} + \frac{1910\pi^2}{243} - \frac{4\pi^4}{15} + \frac{133036}{729} \right) + \frac{428\zeta_5}{9} \right. \\ \left. - \frac{41\pi^2\zeta_3}{27} - \frac{460\zeta_3}{81} + \frac{73\pi^4}{1620} - \frac{14189\pi^2}{4374} - \frac{3765007}{6561} \right] + C_A^3 \left[-\frac{L^6}{6} - \frac{11L^5}{9} \right. \\ \left. + \left(\frac{281}{54} - \frac{\pi^2}{4} \right) L^4 + L^3 \left(2\zeta_3 + \frac{11\pi^2}{18} + \frac{1540}{81} \right) + L^2 \left(\frac{143\zeta_3}{9} + \frac{685\pi^2}{108} - \frac{6740}{81} - \frac{73\pi^4}{360} \right) \right. \\ \left. + L \left(\frac{17\pi^2\zeta_3}{9} + \frac{2048\zeta_3}{27} + 16\zeta_5 + \frac{44\pi^4}{45} - \frac{6710\pi^2}{243} - \frac{373975}{1458} \right) + \frac{2222\zeta_5}{9} \right]$$

$$\begin{aligned}
& -\frac{104\zeta_3^2}{9} - \frac{605\pi^2\zeta_3}{54} - \frac{152716\zeta_3}{243} + \frac{105617\pi^2}{4374} - \frac{1939\pi^4}{9720} + \frac{29639273}{26244} - \frac{24389\pi^6}{408240} \Big] \\
& + n_f^2 C_F \left[\frac{4L^2}{3} + L \left(\frac{32\zeta_3}{3} - \frac{52}{3} \right) - \frac{112\zeta_3}{3} - \frac{10\pi^2}{27} + \frac{4481}{81} - \frac{4\pi^4}{405} \right] \\
& + n_f C_F^2 \left[-2L + \frac{296\zeta_3}{3} - 160\zeta_5 + \frac{304}{9} \right], \tag{B.3}
\end{aligned}$$

and the quark channel coefficients are given by [60]

$$\begin{aligned}
C_S^{q(0)} &= 1, \\
C_S^{q(1)} &= \frac{1}{6} (-6L^2 + \pi^2 - 12) C_F, \\
C_S^{q(2)} &= C_F^2 \left[\frac{L^4}{2} + \left(2 - \frac{\pi^2}{6} \right) L^2 + 6(4L - 5)\zeta_3 - 2\pi^2 L + \frac{7\pi^2}{3} - \frac{83\pi^4}{360} + 6 \right] \\
& + C_F \left[\frac{11L^3 C_A}{9} + \frac{1}{3} \pi^2 L^2 C_A - \frac{67L^2 C_A}{9} - 26L\zeta_3 C_A + \frac{11}{9} \pi^2 L C_A + \frac{242L C_A}{27} + \right. \\
& \left. \frac{151\zeta_3 C_A}{9} + \frac{11\pi^4 C_A}{45} - \frac{467C_A}{81} - \frac{103\pi^2 C_A}{108} - \frac{10L^3}{9} + \frac{50L^2}{9} - \frac{10\pi^2 L}{9} - \frac{280L}{27} + \frac{10\zeta_3}{9} \right. \\
& \left. + \frac{25\pi^2}{54} + \frac{1000}{81} \right], \\
C_S^{q(3)} &= C_F^3 \left[-\frac{L^6}{6} + \frac{\pi^2 L^4}{12} - L^4 - 24L^3 \zeta_3 + 2\pi^2 L^3 + 30L^2 \zeta_3 + \frac{83\pi^4 L^2}{360} - \frac{7\pi^2 L^2}{3} - 6L^2 \right. \\
& - 240L\zeta_5 - \frac{4}{3} \pi^2 L \zeta_3 + 20L\zeta_3 + \frac{19\pi^4 L}{15} + 7\pi^2 L - 50L + 16\zeta_3^2 + \frac{89\pi^2 \zeta_3}{3} \\
& - 654\zeta_3 + 424\zeta_5 + \frac{37729\pi^6}{136080} + \frac{575}{3} - \frac{353\pi^2}{18} - \frac{77\pi^4}{36} \Big] + C_F^2 C_A \left[-\frac{11L^5}{9} - \frac{\pi^2 L^4}{3} \right. \\
& + \frac{67L^4}{9} + 26L^3 \zeta_3 - \frac{308L^3}{27} - \frac{55\pi^2 L^3}{54} - \frac{943L^2 \zeta_3}{9} + \frac{689\pi^2 L^2}{108} + \frac{1673L^2}{81} - \frac{17\pi^4 L^2}{90} \\
& - \frac{5}{3} \pi^2 L \zeta_3 + \frac{1660L\zeta_3}{3} + 120L\zeta_5 + \frac{\pi^4 L}{6} + \frac{614L}{27} - \frac{3506\pi^2 L}{81} + \frac{296\zeta_3^2}{3} - \frac{1676\zeta_5}{9} \\
& - \frac{4820\zeta_3}{27} - \frac{3049\pi^2 \zeta_3}{54} + \frac{31819\pi^2}{486} - \frac{9335}{81} - \frac{893\pi^4}{9720} - \frac{3169\pi^6}{17010} \Big] + C_F \left[\frac{10L^5}{9} - \frac{50L^4}{9} \right. \\
& + \frac{25\pi^2 L^3}{27} + \frac{250L^3}{27} + \frac{350L^2 \zeta_3}{9} - \frac{335\pi^2 L^2}{54} + \frac{3625L^2}{162} - \frac{4160L\zeta_3}{9} + \frac{7\pi^4 L}{9} + \frac{2200\pi^2 L}{81} \\
& - \frac{7075L}{54} + \frac{59980\zeta_3}{81} - \frac{2080\zeta_5}{9} - \frac{95\pi^2 \zeta_3}{27} - \frac{305\pi^4}{972} - \frac{30655\pi^2}{972} + \frac{179375}{972} \Big] \\
& + C_F C_A^2 \left[-\frac{121L^4}{54} - \frac{22\pi^2 L^3}{27} + \frac{1780L^3}{81} + 88L^2 \zeta_3 + \frac{13\pi^2 L^2}{27} - \frac{11\pi^4 L^2}{45} - \frac{11939L^2}{162} \right. \\
& + \frac{44}{9} \pi^2 L \zeta_3 + 136L\zeta_5 - \frac{13900L\zeta_3}{27} + \frac{4822\pi^2 L}{243} - \frac{47\pi^4 L}{54} + \frac{10289L}{1458} + \frac{163\pi^2 \zeta_3}{9} \\
& + \frac{107648\zeta_3}{243} + \frac{106\zeta_5}{9} - \frac{1136\zeta_3^2}{9} + \frac{10093\pi^4}{4860} - \frac{769\pi^6}{5103} - \frac{264515\pi^2}{8748} + \frac{5964431}{26244} \Big] \\
& + C_A C_F \left[\frac{110L^4}{27} + \frac{20\pi^2 L^3}{27} - \frac{2890L^3}{81} - 40L^2 \zeta_3 + \frac{40\pi^2 L^2}{9} + \frac{8635L^2}{81} + \frac{3620L\zeta_3}{9} \right]
\end{aligned}$$

$$\begin{aligned}
& + \frac{11\pi^4 L}{27} - \frac{8180\pi^2 L}{243} - \frac{37495L}{729} + \frac{10\pi^2 \zeta_3}{9} - \frac{20\zeta_5}{3} - \frac{14300\zeta_3}{27} + \frac{166295\pi^2}{4374} \\
& - \frac{119\pi^4}{243} - \frac{2609875}{13122} \Big] + C_F \left[-\frac{50L^4}{27} + \frac{1000L^3}{81} - \frac{100\pi^2 L^2}{27} - \frac{2500L^2}{81} + \frac{400L\zeta_3}{27} \right. \\
& \left. + \frac{1000\pi^2 L}{81} + \frac{23200L}{729} - \frac{5000\zeta_3}{243} - \frac{235\pi^4}{243} - \frac{2650\pi^2}{243} + \frac{51800}{6561} \right], \tag{B.4}
\end{aligned}$$

where $L = \ln [(-m_H^2 - i\epsilon)/\mu^2]$. Although not used in this paper, the fourth-order coefficients can already be extracted from the form factors calculated in Ref. [61] and Ref. [62].

The jet functions are expanded as

$$\tilde{j}^{q,g}(L_J, \mu) = \sum_{n=0} \left(\frac{\alpha_s}{4\pi} \right)^n \tilde{j}^{q,g(n)}(L_J). \tag{B.5}$$

The expansion coefficients for the quark jet function are [12, 71]

$$\begin{aligned}
\tilde{j}^{q(1)}(L_J) &= C_F \left(2L_J^2 - 3L_J - \frac{2\pi^2}{3} + 7 \right), \\
\tilde{j}^{q(2)}(L_J) &= C_F n_f \left[\frac{4}{9} L_J^3 - \frac{29}{9} L_J^2 + \left(\frac{247}{27} - \frac{2\pi^2}{9} \right) L_J + \frac{13\pi^2}{18} - \frac{4057}{324} \right] \\
&+ C_F C_A \left[-\frac{22}{9} L_J^3 + \left(\frac{367}{18} - \frac{2\pi^2}{3} \right) L_J^2 + \left(40\zeta_3 + \frac{11\pi^2}{9} - \frac{3155}{54} \right) L_J - 18\zeta_3 - \frac{37\pi^4}{180} \right. \\
&- \frac{155\pi^2}{36} + \frac{53129}{648} \Big] + C_F^2 \left[2L_J^4 - 6L_J^3 + \left(\frac{37}{2} - \frac{4\pi^2}{3} \right) L_J^2 + \left(4\pi^2 - 24\zeta_3 - \frac{45}{2} \right) L_J \right. \\
&- 6\zeta_3 + \frac{61\pi^4}{90} - \frac{97\pi^2}{12} + \frac{205}{8} \Big], \\
\tilde{j}^{q(3)}(L_J) &= C_F n_f^2 \left[\frac{4}{27} L_J^4 - \frac{116}{81} L_J^3 + \left(\frac{470}{81} - \frac{4\pi^2}{27} \right) L_J^2 + \left(\frac{58\pi^2}{81} - \frac{8714}{729} - \frac{64}{27} \zeta_3 \right) L_J \right] \\
&+ C_F C_A n_f \left[-\frac{44}{27} L_J^4 + \left(\frac{1552}{81} - \frac{8\pi^2}{27} \right) L_J^3 + \left(\frac{28\pi^2}{9} - \frac{7531}{81} + 8\zeta_3 \right) L_J^2 + \left(\frac{32\pi^4}{135} \right. \right. \\
&- \frac{1976\zeta_3}{27} - \frac{2632\pi^2}{243} + \frac{160906}{729} \Big) L_J \Big] + C_F C_A^2 \left[\frac{121}{27} L_J^4 + \left(\frac{44\pi^2}{27} - \frac{4649}{81} \right) L_J^3 + \left(\frac{22\pi^4}{45} \right. \right. \\
&- 132\zeta_3 - \frac{389\pi^2}{27} + \frac{50689}{162} \Big) L_J^2 + \left(\frac{18179\pi^2}{486} - \frac{53\pi^4}{135} - \frac{599375}{729} - 232\zeta_5 - \frac{88\pi^2 \zeta_3}{9} \right. \\
&\left. \left. + \frac{6688\zeta_3}{9} \right) L_J \right] + C_F^2 n_f \left[\frac{8}{9} L_J^5 - \frac{70}{9} L_J^4 + \left(\frac{875}{27} - \frac{20\pi^2}{27} \right) L_J^3 + \left(\frac{151\pi^2}{27} - \frac{15775}{162} \right) L_J^2 \right. \\
&\left. + \left(\frac{32\zeta_3}{9} + \frac{4\pi^4}{27} - \frac{2833\pi^2}{162} + \frac{7325}{36} \right) L_J \right] + C_F^2 C_A \left[-\frac{44}{9} L_J^5 + \left(\frac{433}{9} - \frac{4\pi^2}{3} \right) L_J^4 \right. \\
&\left. + \left(\frac{164\pi^2}{27} - \frac{10537}{54} + 80\zeta_3 \right) L_J^3 + \left(-68\zeta_3 + \frac{\pi^4}{30} - \frac{2045\pi^2}{54} + \frac{157943}{324} \right) L_J^2 \right. \\
&\left. + \left(\frac{290\zeta_3}{3} - 120\zeta_5 - \frac{88\pi^2 \zeta_3}{3} - \frac{923\pi^4}{540} + \frac{35075\pi^2}{324} - \frac{151405}{216} \right) L_J \right] + C_F^3 \left[\frac{4}{3} L_J^6 - 6L_J^5 \right]
\end{aligned}$$

$$\begin{aligned}
& + \left(23 - \frac{4\pi^2}{3}\right)L_J^4 + \left(8\pi^2 - \frac{99}{2} - 48\zeta_3\right)L_J^3 + \left(60\zeta_3 + \frac{61\pi^4}{45} - \frac{151\pi^2}{6} + \frac{349}{4}\right)L_J^2 \\
& + \left(240\zeta_5 + \frac{64\pi^2\zeta_3}{3} - 218\zeta_3 - \frac{149\pi^4}{30} + \frac{145\pi^2}{4} - \frac{815}{8}\right)L_J \Big] + c_{3q}^J, \tag{B.6}
\end{aligned}$$

The scale-independent constant term c_{3q}^J is given by [71]

$$\begin{aligned}
c_{3q}^J = & 25.06777873C_F^3 + 32.81169125C_A C_F^2 - 0.7795843561C_A^2 C_F - 31.65196210C_A C_F n_f T_F \\
& - 61.78995095C_F^2 n_f T_F + 28.49157341C_F n_f^2 T_F^2. \tag{B.7}
\end{aligned}$$

The expansion coefficients for the gluon jet function are [70, 72]

$$\begin{aligned}
\tilde{j}^{g(1)}(L_J) & = C_A \left(2L_J^2 - \frac{11}{3}L_J + \frac{67}{9} - \frac{2\pi^2}{3}\right) + n_f \left(\frac{2}{3}L_J - \frac{10}{9}\right), \\
\tilde{j}^{g(2)}(L_J) & = n_f^2 \left(\frac{4}{9}L_J^2 - \frac{40}{27}L_J - \frac{2\pi^2}{27} + \frac{100}{81}\right) + C_F n_f \left(2L_J + 8\zeta_3 - \frac{55}{6}\right) + C_A n_f \left[\frac{16}{9}L_J^3 \right. \\
& - \frac{28}{3}L_J^2 + \left(\frac{224}{9} - \frac{10\pi^2}{9}\right)L_J - \frac{8\zeta_3}{3} + \frac{67\pi^2}{27} - \frac{760}{27} \Big] + C_A^2 \left[2L_J^4 - \frac{88}{9}L_J^3 + \left(\frac{389}{9} - 2\pi^2\right)L_J^2 \right. \\
& + \left.\left(\frac{55\pi^2}{9} + 16\zeta_3 - \frac{2570}{27}\right)L_J - \frac{88\zeta_3}{3} + \frac{17\pi^4}{36} - \frac{362\pi^2}{27} + \frac{20215}{162}\right], \\
\tilde{j}^{g(3)}(L_J) & = n_f^3 \left[\frac{8}{27}L_J^3 - \frac{40}{27}L_J^2 + \left(\frac{200}{81} - \frac{4\pi^2}{27}\right)L_J\right] + C_F n_f^2 \left[\frac{10}{3}L_J^2 + \left(16\zeta_3 - 24\right)L_J\right] \\
& - C_F^2 n_f L_J + C_A n_f^2 \left[\frac{4}{3}L_J^4 - \frac{292}{27}L_J^3 + \left(\frac{3326}{81} - \frac{4\pi^2}{3}\right)L_J^2 + \left(\frac{508\pi^2}{81} - \frac{116509}{1458} - \frac{256\zeta_3}{27}\right)L_J\right] \\
& + C_A C_F n_f \left[\frac{16}{3}L_J^3 + (32\zeta_3 - 55)L_J^2 + \left(-\frac{8\pi^4}{45} - \frac{10\pi^2}{3} + \frac{5599}{27} - \frac{1096\zeta_3}{9}\right)L_J\right] \\
& + C_A^2 n_f \left[\frac{20}{9}L_J^5 - \frac{64}{3}L_J^4 - \left(\frac{88\pi^2}{27} - \frac{3106}{27}\right)L_J^3 + \left(\frac{586\pi^2}{27} - \frac{8\zeta_3}{3} - \frac{10067}{27}\right)L_J^2 \right. \\
& + \left.\left(\frac{449\pi^4}{270} - \frac{16831\pi^2}{243} + \frac{1052135}{1458} - \frac{1280\zeta_3}{27}\right)L_J\right] + C_A^3 \left[\frac{4}{3}L_J^6 - \frac{110}{9}L_J^5 + \left(85 - \frac{8\pi^2}{3}\right)L_J^4 \right. \\
& + \left.\left(\frac{484\pi^2}{27} - \frac{9623}{27} + 32\zeta_3\right)L_J^3 + \left(\frac{169\pi^4}{90} - \frac{484\zeta_3}{3} - \frac{2362\pi^2}{27} + \frac{85924}{81}\right)L_J^2 \right. \\
& + \left.\left(-\frac{4411\pi^4}{540} + \frac{52678\pi^2}{243} - \frac{1448021}{729} - 112\zeta_5 - \frac{160\pi^2\zeta_3}{9} + \frac{6316\zeta_3}{9}\right)L_J\right] + c_{3g}^J. \tag{B.8}
\end{aligned}$$

From Ref. [72], we have $c_{3g}^J = 647.7843434644$ for $n_f = 5$.

The soft functions are expanded as

$$\tilde{s}_{q,g}(L_S, \mu) = \sum_{n=0} \left(\frac{\alpha_s}{4\pi}\right)^n \tilde{s}^{q,g(n)}(L_S). \tag{B.9}$$

The expansion coefficients for the quark soft function are [12, 80]

$$\begin{aligned}
\tilde{s}^{q(1)}(L_S) &= C_F (-8L_S^2 - \pi^2), \\
\tilde{s}^{q(2)}(L_S) &= C_F n_f \left[-\frac{32}{9}L_S^3 + \frac{80}{9}L_S^2 - \left(\frac{8\pi^2}{9} + \frac{224}{27}\right)L_S - \frac{52\zeta_3}{9} + \frac{77\pi^2}{27} + \frac{40}{81} \right] \\
&\quad + C_F C_A \left[\frac{176}{9}L_S^3 + \left(\frac{8\pi^2}{3} - \frac{536}{9}\right)L_S^2 + \left(\frac{44\pi^2}{9} - 56\zeta_3 + \frac{1616}{27}\right)L_S + \frac{286\zeta_3}{9} + \frac{14\pi^4}{15} \right. \\
&\quad \left. - \frac{871\pi^2}{54} - \frac{2140}{81} \right] + C_F^2 \left(32L_S^4 + 8\pi^2 L_S^2 + \frac{\pi^4}{2} \right), \\
\tilde{s}^{q(3)}(L_S) &= C_F n_f^2 \left[-\frac{64}{27}L_S^4 + \frac{640}{81}L_S^3 - \left(\frac{32\pi^2}{27} + \frac{800}{81}\right)L_S^2 + \left(\frac{64\pi^2}{9} - \frac{3200}{729} - \frac{64\zeta_3}{9}\right)L_S \right] \\
&\quad + C_F C_A n_f \left[\frac{704}{27}L_S^4 + \left(\frac{64\pi^2}{27} - \frac{9248}{81}\right)L_S^3 + \left(\frac{64\pi^2}{9} + \frac{16408}{81}\right)L_S^2 + \left(\frac{6032\zeta_3}{27} + \frac{64\pi^4}{45} \right. \right. \\
&\quad \left. \left. - \frac{19408\pi^2}{243} - \frac{80324}{729} \right)L_S \right] + C_F C_A^2 \left[-\frac{1936}{27}L_S^4 - \left(\frac{352\pi^2}{27} - \frac{28480}{81}\right)L_S^3 + \left(\frac{104\pi^2}{27} \right. \right. \\
&\quad \left. \left. - \frac{88\pi^4}{45} - \frac{62012}{81} + 352\zeta_3 \right)L_S^2 + \left(\frac{50344\pi^2}{243} - \frac{88\pi^4}{9} + \frac{556042}{729} + 384\zeta_5 + \frac{176\pi^2\zeta_3}{9} \right. \right. \\
&\quad \left. \left. - \frac{36272\zeta_3}{27} \right)L_S \right] + C_F^2 n_f \left[\frac{256}{9}L_S^5 - \frac{640}{9}L_S^4 + \left(\frac{32\pi^2}{3} + \frac{1504}{27}\right)L_S^3 + \left(\frac{5620}{81} - \frac{856\pi^2}{27} \right. \right. \\
&\quad \left. \left. - \frac{160\zeta_3}{9} \right)L_S^2 + \left(\frac{608\zeta_3}{9} + \frac{56\pi^4}{45} + \frac{152\pi^2}{27} - \frac{3422}{27}\right)L_S \right] + C_F^2 C_A \left[-\frac{1408}{9}L_S^5 \right. \\
&\quad \left. + \left(\frac{4288}{9} - \frac{64\pi^2}{3}\right)L_S^4 + \left(448\zeta_3 - \frac{176\pi^2}{3} - \frac{12928}{27}\right)L_S^3 + \left(\frac{5092\pi^2}{27} - \frac{2288\zeta_3}{9} - \frac{152\pi^4}{15} \right. \right. \\
&\quad \left. \left. + \frac{17120}{81} \right)L_S^2 + \left(56\pi^2\zeta_3 - \frac{44\pi^4}{9} - \frac{1616\pi^2}{27}\right)L_S \right] + C_F^3 \left[-\frac{256}{3}L_S^6 - 32\pi^2 L_S^4 - 4\pi^4 L_S^2 \right] \\
&\quad + c_{3q}^S. \tag{B.10}
\end{aligned}$$

The three-loop scale-independent term c_{3q}^S is not precisely known at the moment. Its calculation is under active investigation [84, 89, 90]. In Ref. [71], this term was extracted through a numeric fit to the fixed-order thrust distribution. The value (with large uncertainties) reads

$$c_{3q}^S = -19988 \pm 1440(\text{stat.}) \pm 4000(\text{syst.}). \tag{B.11}$$

The results for the gluon soft function can be obtained from the quark one employing the non-Abelian exponential theorem [91–93]. Up to three loops, they are related by the Casimir scaling

$$\ln[\tilde{s}^g(L_S, \mu)] = \frac{C_A}{C_F} \ln[\tilde{s}^q(L_S, \mu)]. \tag{B.12}$$

Hence the expansion coefficients for the gluon soft function are

$$\tilde{s}^{g(1)}(L_S) = C_A (-8L_S^2 - \pi^2),$$

$$\begin{aligned}
\tilde{s}^{g(2)}(L_S) &= C_A n_f \left[-\frac{32}{9} L_S^3 + \frac{80}{9} L_S^2 - \left(\frac{8\pi^2}{9} + \frac{224}{27} \right) L_S + \frac{77\pi^2}{27} + \frac{40}{81} - \frac{52\zeta_3}{9} \right] \\
&+ C_A^2 \left[32 L_S^4 + \frac{176}{9} L_S^3 + \left(\frac{32\pi^2}{3} - \frac{536}{9} \right) L_S^2 + \left(\frac{44\pi^2}{9} + \frac{1616}{27} - 56\zeta_3 \right) L_S + \frac{286\zeta_3}{9} \right. \\
&\left. + \frac{43\pi^4}{30} - \frac{871\pi^2}{54} - \frac{2140}{81} \right], \\
\tilde{s}^{g(3)}(L_S) &= C_A n_f^2 \left[-\frac{64}{27} L_S^4 + \frac{640}{81} L_S^3 - \left(\frac{32\pi^2}{27} + \frac{800}{81} \right) L_S^2 + \left(\frac{64\pi^2}{9} - \frac{3200}{729} - \frac{64\zeta_3}{9} \right) L_S \right] \\
&+ C_F C_A n_f \left[-\frac{32}{3} L_S^3 + \left(\frac{220}{3} - 64\zeta_3 \right) L_S^2 + \left(\frac{608\zeta_3}{9} + \frac{16\pi^4}{45} - \frac{8\pi^2}{3} - \frac{3422}{27} \right) L_S \right] \\
&+ C_A^2 n_f \left[\frac{256}{9} L_S^5 - \frac{1216}{27} L_S^4 + \left(\frac{352\pi^2}{27} - \frac{3872}{81} \right) L_S^3 + \left(\frac{416\zeta_3}{9} - \frac{664\pi^2}{27} + \frac{16088}{81} \right) L_S^2 \right. \\
&+ \left. \left(\frac{6032\zeta_3}{27} + \frac{104\pi^4}{45} - \frac{17392\pi^2}{243} - \frac{80324}{729} \right) L_S \right] + C_A^3 \left[-\frac{256}{3} L_S^6 - \frac{1408}{9} L_S^5 \right. \\
&+ \left. \left(\frac{10928}{27} - \frac{160\pi^2}{3} \right) L_S^4 + \left(448\zeta_3 - \frac{1936\pi^2}{27} - \frac{10304}{81} \right) L_S^3 + \left(\frac{880\zeta_3}{9} - \frac{724\pi^4}{45} \right. \right. \\
&+ \left. \left. \frac{1732\pi^2}{9} - \frac{4988}{9} \right) L_S^2 + \left(\frac{680\pi^2\zeta_3}{9} - \frac{36272\zeta_3}{27} + 384\zeta_5 - \frac{44\pi^4}{3} + \frac{35800\pi^2}{243} \right. \right. \\
&\left. \left. + \frac{556042}{729} \right) L_S \right] + c_{3g}^S, \tag{B.13}
\end{aligned}$$

where

$$\begin{aligned}
c_{3g}^S &= C_A C_F n_f \left(-\frac{52}{9} \pi^2 \zeta_3 + \frac{77\pi^4}{27} + \frac{40\pi^2}{81} \right) + C_A^2 n_f \left(\frac{52\pi^2 \zeta_3}{9} - \frac{77\pi^4}{27} - \frac{40\pi^2}{81} \right) \\
&+ C_A^3 \left(-\frac{286}{9} \pi^2 \zeta_3 - \frac{11\pi^6}{10} + \frac{871\pi^4}{54} + \frac{2140\pi^2}{81} \right) + C_A^2 C_F \left(\frac{286\pi^2 \zeta_3}{9} + \frac{14\pi^6}{15} \right. \\
&\left. - \frac{871\pi^4}{54} - \frac{2140\pi^2}{81} \right) + C_A C_F^2 \frac{1}{6} \pi^6 + \frac{C_A}{C_F} c_{3q}^S. \tag{B.14}
\end{aligned}$$

C Anomalous dimensions

In this Appendix we list the expressions of the various anomalous dimensions appearing in the resummation formula.

For the cusp anomalous dimensions, we write

$$\Gamma_{\text{cusp}}^q(\alpha_s) = C_F [\gamma_{\text{cusp}}(\alpha_s) + \delta\gamma_{\text{cusp}}^q(\alpha_s)], \quad \Gamma_{\text{cusp}}^g(\alpha_s) = C_A [\gamma_{\text{cusp}}(\alpha_s) + \delta\gamma_{\text{cusp}}^g(\alpha_s)]. \tag{C.1}$$

Up to three loops the cusp anomalous dimensions satisfy Casimir scaling, so that $\delta\gamma_{\text{cusp}}^q(\alpha_s)$ and $\delta\gamma_{\text{cusp}}^g(\alpha_s)$ only start at α_s^4 . We define the expansion as

$$\gamma_{\text{cusp}}(\alpha_s) = \sum_{n=0} \gamma_{\text{cusp}}^{(n)} \left(\frac{\alpha_s}{4\pi} \right)^{n+1}, \quad \delta\gamma_{\text{cusp}}^{q,g}(\alpha_s) = \sum_{n=3} \delta\gamma_{\text{cusp}}^{q,g(n)} \left(\frac{\alpha_s}{4\pi} \right)^{n+1} \tag{C.2}$$

The expansion coefficients are [31, 33–35]

$$\begin{aligned}
\gamma_{\text{cusp}}^{(0)} &= 4, \\
\gamma_{\text{cusp}}^{(1)} &= -\frac{1}{3}4\pi^2 C_A + \frac{268C_A}{9} - \frac{80n_f T_F}{9}, \\
\gamma_{\text{cusp}}^{(2)} &= -\frac{16n_f^2}{27} - \frac{208n_f \zeta(3)}{3} + \frac{80\pi^2 n_f}{9} - \frac{1276n_f}{9} + 264\zeta_3 + \frac{44\pi^4}{5} - \frac{536\pi^2}{3} + 1470n_f, \\
\gamma_{\text{cusp}}^{(3)} &= n_f^3 \left(\frac{64\zeta_3}{27} - \frac{32}{81} \right) + n_f^2 \left(\frac{4160\zeta_3}{27} - \frac{304\pi^2}{81} - \frac{104\pi^4}{135} + \frac{17875}{243} \right) + n_f \left(\frac{416\pi^2 \zeta_3}{3} \right. \\
&\quad \left. - \frac{153920\zeta_3}{27} + \frac{19504\zeta_5}{9} + \frac{12800\pi^2}{27} - \frac{616\pi^4}{45} - \frac{344345}{81} \right) - 432\zeta_3^2 - 528\pi^2 \zeta_3 \\
&\quad + 20944\zeta_3 - 10824\zeta_5 + \frac{2706\pi^4}{5} + \frac{84278}{3} - \frac{44200\pi^2}{9} - \frac{2504\pi^6}{105}, \\
\delta\gamma_{\text{cusp}}^{q(3)} &= n_f \left(-\frac{80\zeta_3}{9} - \frac{400\zeta_5}{9} + \frac{40\pi^2}{9} \right) - 720\zeta_3^2 + 80\zeta_3 + 2200\zeta_5 - 40\pi^2 - \frac{124\pi^6}{63}, \\
\delta\gamma_{\text{cusp}}^{g(3)} &= n_f \left(-\frac{80\zeta_3}{3} - \frac{400\zeta_5}{3} + \frac{40\pi^2}{3} \right) - 2160\zeta_3^2 + 240\zeta_3 + 6600\zeta_5 - 120\pi^2 - \frac{124\pi^6}{21}.
\end{aligned} \tag{C.3}$$

As far as we know, there is no complete results for the five-loop cusp anomalous dimensions. In this paper, we make use of the approximate results estimated in [35],

$$\begin{aligned}
\gamma_{\text{cusp}}^{(4)} + \delta\gamma_{\text{cusp}}^{q(4)} &= 50000 \pm 40000, \\
\gamma_{\text{cusp}}^{(4)} + \delta\gamma_{\text{cusp}}^{g(4)} &= 30000 \pm 60000.
\end{aligned} \tag{C.4}$$

The anomalous dimension for the quark Yukawa coupling reads

$$\gamma_y = - \sum_{n=0} \left(\frac{\alpha_s}{4\pi} \right)^{n+1} \gamma_y^{(n)}, \tag{C.5}$$

where [44, 45]

$$\begin{aligned}
\gamma_y^{(0)} &= 6C_F, \\
\gamma_y^{(1)} &= \frac{97C_A C_F}{3} - \frac{10C_F n_f}{3} + 3C_F^2, \\
\gamma_y^{(2)} &= -48\zeta_3 C_A C_F n_f - \frac{556}{27} C_A C_F n_f - \frac{129}{2} C_A C_F^2 + \frac{11413}{54} C_A^2 C_F + 48\zeta_3 C_F^2 n_f \\
&\quad - 46C_F^2 n_f - \frac{70}{27} C_F n_f^2 + 129C_F^3, \\
\gamma_y^{(3)} &= n_f^3 \left(\frac{128\zeta_3}{27} - \frac{664}{243} \right) + n_f^2 \left(\frac{1600\zeta_3}{9} - \frac{32\pi^4}{27} + \frac{10484}{243} \right) + n_f \left(-\frac{68384\zeta_3}{9} \right. \\
&\quad \left. + \frac{36800\zeta_5}{9} + \frac{176\pi^4}{9} - \frac{183446}{27} \right) + \frac{271360\zeta_3}{27} - 17600\zeta_5 + \frac{4603055}{81}.
\end{aligned} \tag{C.6}$$

The anomalous dimension for the Wilson coefficient C_t is

$$\gamma_t(\alpha_s) = \sum_{n=0} \left(\frac{\alpha_s}{4\pi} \right)^{n+1} \gamma_t^{(n)}, \tag{C.7}$$

where [47–51]

$$\begin{aligned}
\gamma_t^{(0)} &= 0, \\
\gamma_t^{(1)} &= \frac{40}{3}C_A n_f T_F - \frac{1}{3}68C_A^2 + 8C_F n_f T_F, \\
\gamma_t^{(2)} &= -\frac{1}{27}650n_f^2 + \frac{10066n_f}{9} - 5714, \\
\gamma_t^{(2)} &= -\frac{2186n_f^3}{243} + n_f^2 \left(-\frac{12944\zeta_3}{27} - \frac{50065}{27} \right) + n_f \left(\frac{13016\zeta_3}{9} + \frac{1078361}{27} \right) \\
&\quad - 21384\zeta_3 - 149753. \tag{C.8}
\end{aligned}$$

The anomalous dimension for the jet functions are

$$\gamma_j^{q,g}(\alpha_s) = \sum_{n=0} \left(\frac{\alpha_s}{4\pi} \right)^{n+1} \gamma_j^{q,g(n)}, \tag{C.9}$$

where [66, 81]

$$\begin{aligned}
\gamma_j^{q(0)} &= -3C_F, \\
\gamma_j^{q(1)} &= \frac{8\pi^2 n_f}{27} + \frac{484n_f}{81} + \frac{352\zeta_3}{3} - \frac{4\pi^2}{3} - \frac{3610}{27}, \\
\gamma_j^{q(2)} &= -\frac{256}{81}\zeta_3 n_f^2 - \frac{14272\zeta_3 n_f}{81} - \frac{80}{243}\pi^2 n_f^2 + \frac{13828n_f^2}{2187} + \frac{1172\pi^4 n_f}{1215} + \frac{1592\pi^2 n_f}{243} \\
&\quad + \frac{100984n_f}{729} - \frac{25696\zeta_5}{9} - \frac{9632\pi^2 \zeta_3}{81} + \frac{153136\zeta(3)}{27} - \frac{6818\pi^4}{405} + \frac{7588\pi^2}{81} \\
&\quad - \frac{470183}{243}, \\
\gamma_j^{q(3)} &= 4483.56,
\end{aligned} \tag{C.10}$$

and [66, 70]

$$\begin{aligned}
\gamma_j^{g(0)} &= -\beta_0, \\
\gamma_j^{g(1)} &= -\frac{2}{9}\pi^2 n_f C_A + \frac{184n_f C_A}{27} + 16\zeta_3 C_A^2 + \frac{11}{9}\pi^2 C_A^2 - \frac{1096C_A^2}{27} + 2n_f C_F, \\
\gamma_j^{g(2)} &= -\frac{304}{9}n_f \zeta_3 C_A C_F - \frac{8}{45}\pi^4 n_f C_A C_F - \frac{2}{3}\pi^2 n_f C_A C_F + \frac{4145}{54}n_f C_A C_F - \frac{112}{27}n_f^2 \zeta_3 C_A \\
&\quad + \frac{1811n_f^2 C_A}{1458} + \frac{20}{81}\pi^2 n_f^2 C_A - \frac{8}{27}n_f \zeta_3 C_A^2 + \frac{77}{135}\pi^4 n_f C_A^2 - \frac{1306}{243}\pi^2 n_f C_A^2 \\
&\quad + \frac{42557n_f C_A^2}{1458} - \frac{64}{9}\pi^2 \zeta_3 C_A^3 + 260\zeta_3 C_A^3 - 112\zeta_5 C_A^3 + \frac{6217}{243}\pi^2 C_A^3 - \frac{583}{270}\pi^4 C_A^3 \\
&\quad - \frac{331153C_A^3}{1458} - \frac{11n_f^2 C_F}{9} - n_f C_F^2, \\
\gamma_j^{g(3)} &= 26138.7.
\end{aligned} \tag{C.11}$$

The hard anomalous dimensions are

$$\gamma_H^{q,g}(\alpha_s) = \sum_{n=0} \left(\frac{\alpha_s}{4\pi} \right)^{n+1} \gamma_H^{q,g(n)}, \tag{C.12}$$

where the coefficients up to three loops can be obtained from Eq. (B.3) and Eq. (B.4). For the gluon case, they read [53–57, 59, 62]

$$\begin{aligned}
\gamma_H^{g(0)} &= 0, \\
\gamma_H^{g(1)} &= -\frac{2\pi^2 n_f}{3} - \frac{152n_f}{9} + 36\zeta_3 + 11\pi^2 - \frac{160}{3}, \\
\gamma_H^{g(2)} &= -\frac{112n_f^2\zeta_3}{9} + \frac{20\pi^2 n_f^2}{27} + \frac{7714n_f^2}{243} + \frac{920n_f\zeta_3}{9} + \frac{214\pi^4 n_f}{45} - \frac{1270\pi^2 n_f}{27} \\
&\quad - \frac{76256n_f}{81} - 120\pi^2\zeta_3 + 2196\zeta_3 - 864\zeta_5 + \frac{6109\pi^2}{9} - \frac{319\pi^4}{5} + \frac{37045}{27}, \\
\gamma_H^{g(3)} &= n_f^3 \left(\frac{400\zeta_3}{81} + \frac{8\pi^2}{81} - \frac{64\pi^4}{405} + \frac{38426}{2187} \right) + n_f^2 \left(\frac{368\pi^2\zeta_3}{9} - \frac{49342\zeta_3}{81} \right. \\
&\quad \left. + \frac{8000\zeta_5}{9} + \frac{19675\pi^2}{486} - \frac{2474\pi^4}{405} + \frac{3605645}{1944} \right) + n_f \left(\frac{32\zeta_3^2}{3} - 504\pi^2\zeta_3 \right. \\
&\quad \left. + \frac{528362\zeta_3}{27} - \frac{90140\zeta_5}{9} + \frac{52153\pi^4}{135} - \frac{262193\pi^2}{162} - \frac{7927313}{216} - \frac{54917\pi^6}{2835} \right) \\
&\quad + 21384\zeta_3^2 + \frac{2004\pi^4\zeta_3}{5} - 576\pi^2\zeta_3 + \frac{119536\zeta_3}{3} + 1152\pi^2\zeta_5 \\
&\quad - 62796\zeta_5 - 22734\zeta_7 + \frac{18051\pi^6}{70} + \frac{1041691\pi^2}{54} - \frac{123029\pi^4}{30} \\
&\quad + \frac{5481844}{81}.
\end{aligned} \tag{C.13}$$

For the quark case, they are given as [53, 60, 61, 94]

$$\begin{aligned}
\gamma_H^{q(0)} &= 0, \\
\gamma_H^{q(1)} &= \frac{8\pi^2 n_f}{9} + \frac{160n_f}{81} + \frac{368\zeta_3}{3} - \frac{68\pi^2}{9} - \frac{352}{27}, \\
\gamma_H^{q(2)} &= -\frac{64n_f^2\zeta_3}{81} - \frac{80\pi^2 n_f^2}{81} + \frac{11776n_f^2}{2187} - \frac{23584n_f\zeta_3}{81} + \frac{136\pi^4 n_f}{1215} + \frac{9128\pi^2 n_f}{243} \\
&\quad - \frac{47192n_f}{729} + \frac{164144\zeta_3}{27} - \frac{30656\zeta_5}{9} - \frac{9760\pi^2\zeta_3}{81} - \frac{10124\pi^2}{81} + \frac{213772}{243} \\
&\quad - \frac{4132\pi^4}{405}, \\
\gamma_H^{q(3)} &= n_f^3 \left(-\frac{2240\zeta_3}{729} - \frac{32\pi^2}{243} - \frac{128\pi^4}{3645} + \frac{95744}{19683} \right) + n_f^2 \left(-\frac{1}{243} 2816\pi^2\zeta_3 \right. \\
&\quad \left. + \frac{18848\zeta_3}{729} + \frac{25984\zeta_5}{81} + \frac{6856\pi^4}{10935} - \frac{130486\pi^2}{2187} + \frac{126461}{4374} \right) + n_f \left(-\frac{110848\zeta_3^2}{27} \right. \\
&\quad \left. + \frac{115504\pi^2\zeta_3}{243} - \frac{3066064\zeta_3}{243} + \frac{59488\zeta_5}{9} + \frac{29264\pi^4}{729} + \frac{755786\pi^2}{729} - \frac{1641457}{486} \right. \\
&\quad \left. - \frac{975668\pi^6}{229635} \right) + \frac{175712\zeta_3^2}{9} + \frac{992696\pi^4\zeta_3}{3645} + \frac{1365152\zeta_3}{9} + \frac{243872\pi^2\zeta_5}{81} \\
&\quad + \frac{2888332\zeta_7}{27} - \frac{81584\pi^2\zeta_3}{9} - \frac{2158832\zeta_5}{9} + \frac{2058794\pi^6}{25515} - \frac{362842\pi^2}{243} \\
&\quad + \frac{19161124}{729} - \frac{1095218\pi^4}{1215}.
\end{aligned} \tag{C.14}$$

Due to the RG invariance of physical observables, the soft anomalous dimensions satisfy the consistency relations

$$\begin{aligned}\gamma_s^q &= \gamma_H^q + \gamma_y - 2\gamma_j^q, \\ \gamma_s^g &= \gamma_H^g + \gamma_t + \frac{\beta}{\alpha_s} - 2\gamma_j^g.\end{aligned}\tag{C.15}$$

We expand them in α_s

$$\gamma_s^{q,g}(\alpha_s) = \sum_{n=0} \left(\frac{\alpha_s}{4\pi}\right)^{n+1} \gamma_s^{q,g(n)},\tag{C.16}$$

where

$$\begin{aligned}\gamma_s^{q(0)} &= 0, \\ \gamma_s^{q(1)} &= \frac{8\pi^2 n_f}{27} - \frac{448n_f}{81} - 112\zeta_3 - \frac{44\pi^2}{9} + \frac{3232}{27}, \\ \gamma_s^{q(2)} &= \frac{448\zeta_3 n_f^2}{81} + \frac{13600\zeta_3 n_f}{81} - \frac{80}{243}\pi^2 n_f^2 - \frac{8320n_f^2}{2187} - \frac{736\pi^4 n_f}{405} + \frac{5944\pi^2 n_f}{243} \\ &\quad - \frac{129496n_f}{729} + 2304\zeta_5 + \frac{352\pi^2 \zeta_3}{3} - 5264\zeta_3 + \frac{352\pi^4}{15} - \frac{25300\pi^2}{81} + \frac{547124}{243}, \\ \gamma_s^{q(3)} &= -5350.4,\end{aligned}\tag{C.17}$$

and

$$\begin{aligned}\gamma_s^{g(0)} &= 0, \\ \gamma_s^{g(1)} &= \frac{2\pi^2 n_f}{3} - \frac{112n_f}{9} - 252\zeta_3 - 11\pi^2 + \frac{808}{3}, \\ \gamma_s^{g(2)} &= \frac{112n_f^2 \zeta_3}{9} - \frac{20\pi^2 n_f^2}{27} - \frac{2080n_f^2}{243} + \frac{3400n_f \zeta_3}{9} + \frac{1486\pi^2 n_f}{27} - \frac{184\pi^4 n_f}{45} \\ &\quad - \frac{32374n_f}{81} + 264\pi^2 \zeta_3 - 11844\zeta_3 + 5184\zeta_5 + \frac{264\pi^4}{5} - \frac{6325\pi^2}{9} + \frac{136781}{27}, \\ \gamma_s^{g(3)} &= -14715.4.\end{aligned}\tag{C.18}$$

Up to three loops, the quark and gluon soft anomalous dimensions satisfy the Casimir scaling $\gamma_s^g/C_A = \gamma_s^q/C_F$. However, starting at four loops, due to the emergence of new Casimir operators, the relation must be generalized as appropriate [66, 95].

Finally, the beta function coefficients are [40, 41]

$$\begin{aligned}
\beta_0 &= \frac{11C_A}{3} - \frac{4n_f T_F}{3}, \\
\beta_1 &= \frac{34C_A^2}{3} - \frac{20C_A n_f T_F}{3} - 4C_F n_f T_F, \\
\beta_2 &= \frac{325n_f^2}{54} - \frac{5033n_f}{18} + \frac{2857}{2}, \\
\beta_3 &= \frac{1093n_f^3}{729} + n_f^2 \left(\frac{6472\zeta_3}{81} + \frac{50065}{162} \right) + n_f \left(-\frac{6508\zeta_3}{27} - \frac{1078361}{162} \right) + 3564\zeta_3 \\
&\quad + \frac{149753}{6}, \\
\beta_4 &= n_f^4 \left(\frac{1205}{2916} - \frac{152\zeta_3}{81} \right) + n_f^3 \left(-\frac{48722\zeta_3}{243} + \frac{460\zeta_5}{9} + \frac{809\pi^4}{1215} - \frac{630559}{5832} \right) \\
&\quad + n_f^2 \left(\frac{698531\zeta_3}{81} - \frac{381760\zeta_5}{81} - \frac{5263\pi^4}{405} + \frac{25960913}{1944} \right) + n_f \left(-\frac{4811164\zeta_3}{81} \right. \\
&\quad \left. + \frac{1358995\zeta_5}{27} + \frac{6787\pi^4}{108} - \frac{336460813}{1944} \right) + \frac{621885\zeta_3}{2} - 288090\zeta_5 + \frac{8157455}{16} \\
&\quad - \frac{9801\pi^4}{20}.
\end{aligned} \tag{C.19}$$

References

- [1] G.F. Giudice and O. Lebedev, *Higgs-dependent Yukawa couplings*, *Phys. Lett. B* **665** (2008) 79 [0804.1753].
- [2] F. Bishara, J. Brod, P. Uttayarat and J. Zupan, *Nonstandard Yukawa Couplings and Higgs Portal Dark Matter*, *JHEP* **01** (2016) 010 [1504.04022].
- [3] ILC collaboration, H. Baer et al., eds., *The International Linear Collider Technical Design Report - Volume 2: Physics*, 1306.6352.
- [4] A. Arbey et al., *Physics at the e^+e^- Linear Collider*, *Eur. Phys. J. C* **75** (2015) 371 [1504.01726].
- [5] CEPC STUDY GROUP collaboration, *CEPC Conceptual Design Report: Volume 2 - Physics & Detector*, 1811.10545.
- [6] P. Bambade et al., *The International Linear Collider: A Global Project*, 1903.01629.
- [7] FCC collaboration, *FCC-ee: The Lepton Collider: Future Circular Collider Conceptual Design Report Volume 2*, *Eur. Phys. J. ST* **228** (2019) 261.
- [8] E. Farhi, *A QCD Test for Jets*, *Phys. Rev. Lett.* **39** (1977) 1587.
- [9] J. Gao, Y. Gong, W.-L. Ju and L.L. Yang, *Thrust distribution in Higgs decays at the next-to-leading order and beyond*, *JHEP* **03** (2019) 030 [1901.02253].
- [10] S. Catani, L. Trentadue, G. Turnock and B.R. Webber, *Resummation of large logarithms in e^+e^- event shape distributions*, *Nucl. Phys. B* **407** (1993) 3.
- [11] M.D. Schwartz, *Resummation and NLO matching of event shapes with effective field theory*, *Phys. Rev. D* **77** (2008) 014026 [0709.2709].
- [12] T. Becher and M.D. Schwartz, *A precise determination of α_s from LEP thrust data using effective field theory*, *JHEP* **07** (2008) 034 [0803.0342].
- [13] G. Dissertori, A. Gehrmann-De Ridder, T. Gehrmann, E.W.N. Glover, G. Heinrich, G. Luisoni et al., *Determination of the strong coupling constant using matched NNLO+NLLA predictions for hadronic event shapes in e^+e^- annihilations*, *JHEP* **08** (2009) 036 [0906.3436].
- [14] R. Abbate, M. Fickinger, A.H. Hoang, V. Mateu and I.W. Stewart, *Thrust at N^3LL with Power Corrections and a Precision Global Fit for $\alpha_s(m_Z)$* , *Phys. Rev. D* **83** (2011) 074021 [1006.3080].
- [15] P.F. Monni, T. Gehrmann and G. Luisoni, *Two-Loop Soft Corrections and Resummation of the Thrust Distribution in the Dijet Region*, *JHEP* **08** (2011) 010 [1105.4560].
- [16] A. Banfi, H. McAslan, P.F. Monni and G. Zanderighi, *A general method for the resummation of event-shape distributions in e^+e^- annihilation*, *JHEP* **05** (2015) 102 [1412.2126].
- [17] A.H. Hoang, D.W. Kolodrubetz, V. Mateu and I.W. Stewart, *C -parameter distribution at N^3LL' including power corrections*, *Phys. Rev. D* **91** (2015) 094017 [1411.6633].
- [18] G. Bell, A. Hornig, C. Lee and J. Talbert, *e^+e^- angularity distributions at NNLL' accuracy*, *JHEP* **01** (2019) 147 [1808.07867].
- [19] J. Mo, F.J. Tackmann and W.J. Waalewijn, *A case study of quark-gluon discrimination at NNLL' in comparison to parton showers*, *Eur. Phys. J. C* **77** (2017) 770 [1708.00867].

- [20] S. Alioli, A. Broggio, A. Gavardi, S. Kallweit, M.A. Lim, R. Nagar et al., *Resummed predictions for hadronic Higgs boson decays*, *JHEP* **04** (2021) 254 [[2009.13533](#)].
- [21] S. Catani, G. Turnock, B.R. Webber and L. Trentadue, *Thrust distribution in e^+e^- annihilation*, *Phys. Lett. B* **263** (1991) 491.
- [22] H. Contopanagos, E. Laenen and G.F. Sterman, *Sudakov factorization and resummation*, *Nucl. Phys. B* **484** (1997) 303 [[hep-ph/9604313](#)].
- [23] N. Kidonakis, G. Oderda and G.F. Sterman, *Threshold resummation for dijet cross-sections*, *Nucl. Phys. B* **525** (1998) 299 [[hep-ph/9801268](#)].
- [24] C.F. Berger, T. Kucs and G.F. Sterman, *Event shape / energy flow correlations*, *Phys. Rev. D* **68** (2003) 014012 [[hep-ph/0303051](#)].
- [25] C.W. Bauer, S. Fleming and M.E. Luke, *Summing Sudakov logarithms in $B \rightarrow X_s \gamma$ in effective field theory.*, *Phys. Rev. D* **63** (2000) 014006 [[hep-ph/0005275](#)].
- [26] C.W. Bauer, S. Fleming, D. Pirjol and I.W. Stewart, *An Effective field theory for collinear and soft gluons: Heavy to light decays*, *Phys. Rev. D* **63** (2001) 114020 [[hep-ph/0011336](#)].
- [27] C.W. Bauer and I.W. Stewart, *Invariant operators in collinear effective theory*, *Phys. Lett. B* **516** (2001) 134 [[hep-ph/0107001](#)].
- [28] C.W. Bauer, S. Fleming, D. Pirjol, I.Z. Rothstein and I.W. Stewart, *Hard scattering factorization from effective field theory*, *Phys. Rev. D* **66** (2002) 014017 [[hep-ph/0202088](#)].
- [29] C.W. Bauer, D. Pirjol and I.W. Stewart, *Soft collinear factorization in effective field theory*, *Phys. Rev. D* **65** (2002) 054022 [[hep-ph/0109045](#)].
- [30] M. Beneke, A.P. Chapovsky, M. Diehl and T. Feldmann, *Soft collinear effective theory and heavy to light currents beyond leading power*, *Nucl. Phys. B* **643** (2002) 431 [[hep-ph/0206152](#)].
- [31] S. Moch, J.A.M. Vermaseren and A. Vogt, *The Three loop splitting functions in QCD: The Nonsinglet case*, *Nucl. Phys. B* **688** (2004) 101 [[hep-ph/0403192](#)].
- [32] A. Vogt, S. Moch and J.A.M. Vermaseren, *The Three-loop splitting functions in QCD: The Singlet case*, *Nucl. Phys. B* **691** (2004) 129 [[hep-ph/0404111](#)].
- [33] J.M. Henn, G.P. Korchemsky and B. Mistlberger, *The full four-loop cusp anomalous dimension in $\mathcal{N} = 4$ super Yang-Mills and QCD*, *JHEP* **04** (2020) 018 [[1911.10174](#)].
- [34] A. von Manteuffel, E. Panzer and R.M. Schabinger, *Cusp and collinear anomalous dimensions in four-loop QCD from form factors*, *Phys. Rev. Lett.* **124** (2020) 162001 [[2002.04617](#)].
- [35] F. Herzog, S. Moch, B. Ruijl, T. Ueda, J.A.M. Vermaseren and A. Vogt, *Five-loop contributions to low- N non-singlet anomalous dimensions in QCD*, *Phys. Lett. B* **790** (2019) 436 [[1812.11818](#)].
- [36] W.E. Caswell, *Asymptotic Behavior of Nonabelian Gauge Theories to Two Loop Order*, *Phys. Rev. Lett.* **33** (1974) 244.
- [37] D.R.T. Jones, *Two Loop Diagrams in Yang-Mills Theory*, *Nucl. Phys. B* **75** (1974) 531.
- [38] O.V. Tarasov, A.A. Vladimirov and A.Y. Zharkov, *The Gell-Mann-Low Function of QCD in the Three Loop Approximation*, *Phys. Lett. B* **93** (1980) 429.

- [39] S.A. Larin and J.A.M. Vermaseren, *The Three loop QCD Beta function and anomalous dimensions*, *Phys. Lett. B* **303** (1993) 334 [[hep-ph/9302208](#)].
- [40] T. van Ritbergen, J.A.M. Vermaseren and S.A. Larin, *The Four loop beta function in quantum chromodynamics*, *Phys. Lett. B* **400** (1997) 379 [[hep-ph/9701390](#)].
- [41] M. Czakon, *The Four-loop QCD beta-function and anomalous dimensions*, *Nucl. Phys. B* **710** (2005) 485 [[hep-ph/0411261](#)].
- [42] R. Tarrach, *The Pole Mass in Perturbative QCD*, *Nucl. Phys. B* **183** (1981) 384.
- [43] S.A. Larin, *The Renormalization of the axial anomaly in dimensional regularization*, *Phys. Lett. B* **303** (1993) 113 [[hep-ph/9302240](#)].
- [44] J.A.M. Vermaseren, S.A. Larin and T. van Ritbergen, *The four loop quark mass anomalous dimension and the invariant quark mass*, *Phys. Lett. B* **405** (1997) 327 [[hep-ph/9703284](#)].
- [45] K.G. Chetyrkin, *Quark mass anomalous dimension to $O(\alpha_s^4)$* , *Phys. Lett. B* **404** (1997) 161 [[hep-ph/9703278](#)].
- [46] P.A. Baikov, K.G. Chetyrkin and J.H. Kühn, *Quark Mass and Field Anomalous Dimensions to $O(\alpha_s^5)$* , *JHEP* **10** (2014) 076 [[1402.6611](#)].
- [47] V.P. Spiridonov, *Anomalous Dimension of $G_{\mu\nu}^2$ and β Function*, .
- [48] M. Kramer, E. Laenen and M. Spira, *Soft gluon radiation in Higgs boson production at the LHC*, *Nucl. Phys. B* **511** (1998) 523 [[hep-ph/9611272](#)].
- [49] K.G. Chetyrkin, B.A. Kniehl and M. Steinhauser, *Decoupling relations to $O(\alpha_s^3)$ and their connection to low-energy theorems*, *Nucl. Phys. B* **510** (1998) 61 [[hep-ph/9708255](#)].
- [50] Y. Schroder and M. Steinhauser, *Four-loop decoupling relations for the strong coupling*, *JHEP* **01** (2006) 051 [[hep-ph/0512058](#)].
- [51] K.G. Chetyrkin, J.H. Kuhn and C. Sturm, *QCD decoupling at four loops*, *Nucl. Phys. B* **744** (2006) 121 [[hep-ph/0512060](#)].
- [52] T. Liu and M. Steinhauser, *Decoupling of heavy quarks at four loops and effective Higgs-fermion coupling*, *Phys. Lett. B* **746** (2015) 330 [[1502.04719](#)].
- [53] S. Dawson, *Radiative corrections to Higgs boson production*, *Nucl. Phys. B* **359** (1991) 283.
- [54] A. Djouadi, M. Spira and P.M. Zerwas, *Production of Higgs bosons in proton colliders: QCD corrections*, *Phys. Lett. B* **264** (1991) 440.
- [55] R.V. Harlander, *Virtual corrections to $g g \rightarrow H$ to two loops in the heavy top limit*, *Phys. Lett. B* **492** (2000) 74 [[hep-ph/0007289](#)].
- [56] S. Moch, J.A.M. Vermaseren and A. Vogt, *Three-loop results for quark and gluon form-factors*, *Phys. Lett. B* **625** (2005) 245 [[hep-ph/0508055](#)].
- [57] T. Gehrmann, T. Huber and D. Maitre, *Two-loop quark and gluon form-factors in dimensional regularisation*, *Phys. Lett. B* **622** (2005) 295 [[hep-ph/0507061](#)].
- [58] P.A. Baikov, K.G. Chetyrkin, A.V. Smirnov, V.A. Smirnov and M. Steinhauser, *Quark and gluon form factors to three loops*, *Phys. Rev. Lett.* **102** (2009) 212002 [[0902.3519](#)].
- [59] T. Gehrmann, E.W.N. Glover, T. Huber, N. Ikizlerli and C. Studerus, *Calculation of the quark and gluon form factors to three loops in QCD*, *JHEP* **06** (2010) 094 [[1004.3653](#)].

- [60] T. Gehrmann and D. Kara, *The $Hb\bar{b}$ form factor to three loops in QCD*, *JHEP* **09** (2014) 174 [[1407.8114](#)].
- [61] A. Chakraborty, T. Huber, R.N. Lee, A. von Manteuffel, R.M. Schabinger, A.V. Smirnov et al., *$Hb\bar{b}$ vertex at four loops and hard matching coefficients in SCET for various currents*, *Phys. Rev. D* **106** (2022) 074009 [[2204.02422](#)].
- [62] R.N. Lee, A. von Manteuffel, R.M. Schabinger, A.V. Smirnov, V.A. Smirnov and M. Steinhauser, *Quark and Gluon Form Factors in Four-Loop QCD*, *Phys. Rev. Lett.* **128** (2022) 212002 [[2202.04660](#)].
- [63] G.P. Korchemsky and G. Marchesini, *Resummation of large infrared corrections using Wilson loops*, *Phys. Lett. B* **313** (1993) 433.
- [64] A.V. Belitsky, *Two loop renormalization of Wilson loop for Drell-Yan production*, *Phys. Lett. B* **442** (1998) 307 [[hep-ph/9808389](#)].
- [65] Y. Li, A. von Manteuffel, R.M. Schabinger and H.X. Zhu, *Soft-virtual corrections to Higgs production at N^3LO* , *Phys. Rev. D* **91** (2015) 036008 [[1412.2771](#)].
- [66] C. Duhr, B. Mistlberger and G. Vita, *Soft integrals and soft anomalous dimensions at N^3LO and beyond*, *JHEP* **09** (2022) 155 [[2205.04493](#)].
- [67] C.W. Bauer and A.V. Manohar, *Shape function effects in $B \rightarrow X(s) \gamma$ and $B \rightarrow X(u) l \bar{\nu}$ decays*, *Phys. Rev. D* **70** (2004) 034024 [[hep-ph/0312109](#)].
- [68] S.W. Bosch, B.O. Lange, M. Neubert and G. Paz, *Factorization and shape function effects in inclusive B meson decays*, *Nucl. Phys. B* **699** (2004) 335 [[hep-ph/0402094](#)].
- [69] T. Becher and M. Neubert, *Toward a NNLO calculation of the anti-B $\rightarrow X(s) \gamma$ decay rate with a cut on photon energy. II. Two-loop result for the jet function*, *Phys. Lett. B* **637** (2006) 251 [[hep-ph/0603140](#)].
- [70] T. Becher and M.D. Schwartz, *Direct photon production with effective field theory*, *JHEP* **02** (2010) 040 [[0911.0681](#)].
- [71] R. Brüser, Z.L. Liu and M. Stahlhofen, *Three-Loop Quark Jet Function*, *Phys. Rev. Lett.* **121** (2018) 072003 [[1804.09722](#)].
- [72] P. Banerjee, P.K. Dhani and V. Ravindran, *Gluon jet function at three loops in QCD*, *Phys. Rev. D* **98** (2018) 094016 [[1805.02637](#)].
- [73] T. Becher and G. Bell, *The gluon jet function at two-loop order*, *Phys. Lett. B* **695** (2011) 252 [[1008.1936](#)].
- [74] T. Inami, T. Kubota and Y. Okada, *Effective Gauge Theory and the Effect of Heavy Quarks in Higgs Boson Decays*, *Z. Phys. C* **18** (1983) 69.
- [75] A. Djouadi, J. Kalinowski and P.M. Zerwas, *Higgs radiation off top quarks in high-energy e^+e^- colliders*, *Z. Phys. C* **54** (1992) 255.
- [76] K.G. Chetyrkin, B.A. Kniehl and M. Steinhauser, *Hadronic Higgs decay to order α_s^{*4}* , *Phys. Rev. Lett.* **79** (1997) 353 [[hep-ph/9705240](#)].
- [77] P.A. Baikov, K.G. Chetyrkin and J.H. Kühn, *Five-Loop Running of the QCD coupling constant*, *Phys. Rev. Lett.* **118** (2017) 082002 [[1606.08659](#)].
- [78] T. Ahmed, M. Mahakhud, P. Mathews, N. Rana and V. Ravindran, *Two-loop QCD corrections to $Higgs \rightarrow b + \bar{b} + g$ amplitude*, *JHEP* **08** (2014) 075 [[1405.2324](#)].

- [79] S. Fleming, A.H. Hoang, S. Mantry and I.W. Stewart, *Top Jets in the Peak Region: Factorization Analysis with NLL Resummation*, *Phys. Rev. D* **77** (2008) 114003 [0711.2079].
- [80] R. Kelley, M.D. Schwartz, R.M. Schabinger and H.X. Zhu, *The two-loop hemisphere soft function*, *Phys. Rev. D* **84** (2011) 045022 [1105.3676].
- [81] T. Becher, M. Neubert and B.D. Pecjak, *Factorization and Momentum-Space Resummation in Deep-Inelastic Scattering*, *JHEP* **01** (2007) 076 [hep-ph/0607228].
- [82] S. Catani, M.L. Mangano, P. Nason and L. Trentadue, *The Resummation of soft gluons in hadronic collisions*, *Nucl. Phys. B* **478** (1996) 273 [hep-ph/9604351].
- [83] PARTICLE DATA GROUP collaboration, *Review of Particle Physics*, *Phys. Rev. D* **98** (2018) 030001.
- [84] D. Baranowski, M. Delto, K. Melnikov and C.-Y. Wang, *Same-hemisphere three-gluon-emission contribution to the zero-jettiness soft function at N³LO QCD*, *Phys. Rev. D* **106** (2022) 014004 [2204.09459].
- [85] W. Chen, F. Feng, Y. Jia and X. Liu, *Double-real-virtual and double-virtual-real corrections to the three-loop thrust soft function*, *JHEP* **22** (2020) 094 [2206.12323].
- [86] T. Becher and M. Neubert, *Threshold resummation in momentum space from effective field theory*, *Phys. Rev. Lett.* **97** (2006) 082001 [hep-ph/0605050].
- [87] L.G. Almeida, S.D. Ellis, C. Lee, G. Sterman, I. Sung and J.R. Walsh, *Comparing and counting logs in direct and effective methods of QCD resummation*, *JHEP* **04** (2014) 174 [1401.4460].
- [88] D. Bertolini, M.P. Solon and J.R. Walsh, *Integrated and Differential Accuracy in Resummed Cross Sections*, *Phys. Rev. D* **95** (2017) 054024 [1701.07919].
- [89] W. Chen, F. Feng, Y. Jia and X. Liu, *Double-real-virtual and double-virtual-real corrections to the three-loop thrust soft function*, *JHEP* **22** (2020) 094 [2206.12323].
- [90] D. Baranowski, M. Delto, K. Melnikov and C.-Y. Wang, *On phase-space integrals with Heaviside functions*, *JHEP* **02** (2022) 081 [2111.13594].
- [91] G.F. Sterman, *Infrared divergences in perturbative QCD*, *AIP Conf. Proc.* **74** (1981) 22.
- [92] J.G.M. Gatheral, *Exponentiation of Eikonal Cross-sections in Nonabelian Gauge Theories*, *Phys. Lett. B* **133** (1983) 90.
- [93] J. Frenkel and J.C. Taylor, *NONABELIAN EIKONAL EXPONENTIATION*, *Nucl. Phys. B* **246** (1984) 231.
- [94] R.V. Harlander and W.B. Kilgore, *Higgs boson production in bottom quark fusion at next-to-next-to leading order*, *Phys. Rev. D* **68** (2003) 013001 [hep-ph/0304035].
- [95] S. Moch, B. Ruijl, T. Ueda, J.A.M. Vermaseren and A. Vogt, *On quartic colour factors in splitting functions and the gluon cusp anomalous dimension*, *Phys. Lett. B* **782** (2018) 627 [1805.09638].